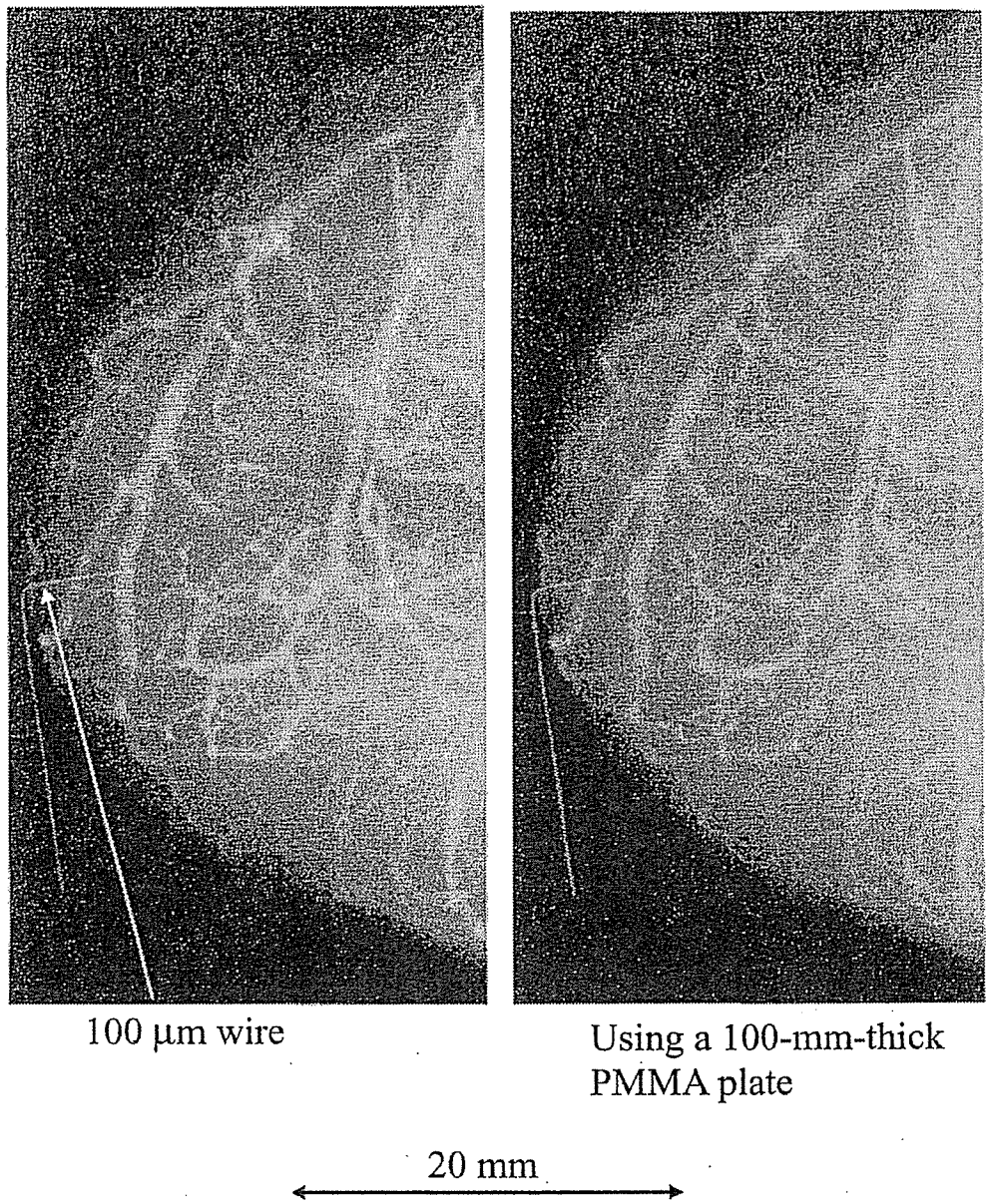

Fig. 17. Magnification angiograms of a dog heart.

7. おわりに

低フォトンエネルギープラズマX線装置では充電電圧の増加により，高調波が観測された。これらの高調波は制動X線のプラズマ内での吸収により発生したと思われる。要するに，K系列特性X線の整数倍のフォトンエネルギーに相当する制動線がプラズマを透過し易いと想像される。次にモリブデン管付き高フォトンエネルギープラズマX線装置ではジルコニウムフィルターにより Kβ線が吸収され難く，この現象は Kβ線の線吸収係数が低下したためと思われる。

セリウムX線装置から発生するK系列特性X線はシャープで，前述のように硫酸バリウムのフィル

ターを用いた場合にはKα線を有効に用いることができる。しかしKβ線も効率よく吸収されることから，酸化セリウムのフィルターも有用であると思われる。現在，回転陽極管を製作するための基礎実験を行っており，高線量率セリウム管も実現するかもしれない。

血管のコントラストは若干劣るが，アルミニウムフィルター等を使って発生する疑似単色制動X線も有効であった。さらに被曝線量を考慮する必要はあるが，拡大撮影による空間分解能の向上，散乱線の低減，そして位相コントラスト効果の付加は，これからのデジタル撮影には必須であると思われる。100 W級の10 μmフォーカス回転陽極管が実用化され，加えてkW級の100 μmフォーカス管は製作可能であることから，特に高精細撮影を行う場合には小焦点管をお勧めする。

謝辞

本研究は文部科学省，厚生労働省，私学振興財団，JST，NEDO，そして岩手県からの研究助成金により遂行されている。

文献

1. J.J. Rocca, V. Shlyaptsev, F.G. Tomasel, O.D.Cortazar, D. Hartshorn and J.L.A. Chilla, "Demonstration of a discharge pumped table-top soft x-ray laser," *Phys. Lev. Lett.*, **73**, 2192-2195, 1994.

2. K. Yoshiaki, A. Nagashima, K. Nagashima, M. Kado, T. Kawachi, N. Hasegawa, M. Tanaka, A. Sasaki and K. Moribayashi, "X-ray lasers driven by optical lasers," *AIP Conference Proc.*, **506**, 613-620, 1999.

3. J.J.G. Rocca, J.L.A. Chilla, S. Sakadzic, A. Rahman, J. Filevich, E. Jankowska, E.C. Hammarsten, B.M. Luther, H.C. Kapteyn, M. Murnane and V.N. Shlyapsev, "Advances in capillary discharge soft x-ray laser research," *SPIE*, **4505**, 1-6, 2001.

4. S. Le Pape, Ph. Zeitoun, J.J.G. Rocca, A. Carillon, P. Dhez, M. Francois, S. Hubert, M. Idir and D. Ros, "Characterisation of an x-ray laser beam," *SPIE*, **4505**, 23-34, 2001.

5. C. Gerth, "Free-electron laser at the TESLA test facility at DESY: toward a tunable short-pulsed soft x-ray source," *SPIE*, **4505**, 131-145, 2001.

6. A. C. Thompson, H. D. Zeman, G. S. Brown, J. Morrison, P. Reiser, V. Padmanabahn, L. Ong, S. Green, J. Giacomini, H. Gordon and E. Rubenstein, "First operation of the medical research facility at the NSLS for coronary angiography," *Rev. Sci. Instrum.*, **63**, 625-628, 1992.

7. H. Mori, K. Hyodo, E. Tanaka, M. U. Mohammed, A. Yamakawa, Y. Shinozaki, H. Nakazawa, Y. Tanaka, T. Sekka, Y. Iwata, S. Honda, K. Umetani, H. Ueki, T. Yokoyama, K. Tanioka, M. Kubota, H. Hosaka, N. Ishizawa and M. Ando, "Small-vessel radiography in situ with monochromatic synchrotoron radiation," *Radiology*, **201**, 173-177, 1996.

8. K. Hyodo, M. Ando, Y. Oku, S. Yamamoto, T. Takeda, Y. Itai, S. Ohtsuka, Y. Sugishita and J. Tada, "Development of a two-dimensional imaging system for clinical applications of intravenous coronary angiography using intense synchrotron radiation produced by a multipole wiggler," *J. Synchrotron Radiat.*, **5**, 1123-1126, 1998.

9. T. J. Davis, D. Gao, T. E. Gureyev, A. W. Stevenson and S. W. Wilkins, "Phase-contrast imaging of weakly absorbing materials using hard x-rays," *Nature*, **373**, 595-597, 1995.

10. A. Momose, T. Takeda, Y. Itai and K. Hirano, "Phase-contrast x-ray computed tomography for observing

biological soft tissues," *Nature Medicine*, **2**, 473-475, 1996.

11. M. Ando, A. Maksimenko, H. Sugiyama, W. Pattanasiriwisawa, K. Hyodo and C. Uyama, "A simple x-ray dark-and bright-field imaging using achromatic Laue optics," *Jpn. J. Appl. Phys.*, **41**, L1016-L1018, 2002.

12. S. W. Wilkins, T. E. Gureyev, D. Gao, A. Pogany and A. W. Stevenson, "Phase-contrast imaging using polychromatic hard x-rays," *Nature*, 384, 335-338, 1996.

13. A. Ishisaka, H. Ohara and C. Honda, "A new method of analyzing edge effect in phase contrast imaging with incoherent x-rays," *Opt. Rev.*, **7**, 566-572, 2000.

14. H. Ohara. C. Honda, A. Ishisaka and F. Shimoda, "Image quality in digital phase contrast imaging using a tungsten anode x-ray tube with a small focal spot size," *SPIE*, **4682**, 1-11, 2002.

15. E. Sato, K. Sato, T. Usuki and Y. Tamakawa, "Film-less computed radiography system for high-speed imaging," *Ann. Rep. Iwate Med. Univ. Sch. Lib. Arts and Sci.*, **35**, 13-23, 2000.

16. E. Sato, Y. Hayasi, R. Germer, E. Tanaka, H. Mori, T. Kawai, H. Obara, T. Ichimaru, K. Takayama and H. Ido, "Intense characteristic x-ray irradiation from weakly ionized linear plasma and applications," *Jpn. J. Med. Imag. Inform. Sci.*, **20**, 148-155, 2003.

17. E. Sato, Y. Hayasi, R. Germer, E. Tanaka, H. Mori, T. Kawai, H. Obara, T. Ichimaru, K. Takayama and H. Ido, "Irradiation of intense characteristic x-rays from weakly ionized linear molybdenum plasma," *Jpn. J. Med. Phys.*, **23**, 123-131, 2003.

18. E. Sato, Y. Hayasi, R. Germer, E. Tanaka, H. Mori, T. Kawai, T. Ichimaru, K. Takayama and H. Ido, "Quasi-monochromatic flash x-ray generator utilizing weakly ionized linear copper plasma," *Rev. Sci. Instrum.*, **74**, 5236-5240, 2003.

19. E. Sato, Y. Hayasi, R. Germer, E. Tanaka, H. Mori, T. Kawai, T. Ichimaru, S. Sato, K. Takayama and H. Ido, "Sharp characteristic x-ray irradiation from weakly ionized linear plasma," *J. Electron Spectrosc. Related Phenom.*, **137-140**, 713-720, 2004.

20. E. Sato, E. Tanaka, H. Mori, T. Kawai,S. Sato and K. Takayama, "Clean monochromatic x-ray irradiation from weakly ionized linear copper plasma," *Opt. Eng.*, **44**, 049002-1-6, 2005.

21. E. Sato, M. Sagae, E. Tanaka, Y. Hayasi, R. Germer, H. Mori, T. Kawai, T. Ichimaru, S. Sato, K. Takayama and H. Ido, "Quasi-monochromatic flash x-ray generator utilizing a disk-cathode molybdenum tube," *Jpn. J. Appl. Phys.*, **43**, 7324-7328, 2004.

22. E. Sato, E. Tanaka, H. Mori, T. Kawai, T. Ichimaru, S. Sato, K. Takayama and H. Ido, "Compact monochromatic flash x-ray generator utilizing a disk-cathode molybdenum tube," *Med. Phys.*, **32**, 49-54, 2005.

23. E. Sato, E. Tanaka, H. Mori, T. Kawai, T. Inoue, A. Ogawa, S. Sato, K. Takayama and H. Ido, "High-speed K-edge angiography achieved with tantalum K-series characteristic x rays," *SPIE*, **5745**, 810-817, 2005.

24. E. Sato, Y. Hayasi, R. Germer, E. Tanaka, H. Mori, T. Kawai, T. Ichimaru, S. Sato, K. Takayama and H. Ido, "Portable x-ray generator utilizing a cerium-target radiation tube for angiography," *J. Electron Spectrosc. Related Phenom.*, **137-140**, 699-704, 2004.

25. E. Sato, E. Tanaka, H. Mori, T. Kawai, T. Ichimaru, S. Sato, K. Takayama and H. Ido, "Demonstration of enhanced K-edge angiography using a cerium target x-ray generator," *Med. Phys*, **31**, 3017-3021, 2004.

Article

A novel LIM protein Cal promotes cardiac differentiation by association with CSX/NKX2-5

Hiroshi Akazawa,[1] Sumiyo Kudoh,[2] Naoki Mochizuki,[3] Noboru Takekoshi,[2] Hiroyuki Takano,[1] Toshio Nagai,[1] and Issei Komuro[1]

[1]Department of Cardiovascular Science and Medicine, Chiba University Graduate School of Medicine, Chiba 260-8670, Japan
[2]Department of Cardiology, Kanazawa Medical University, Ishikawa 920-0265, Japan
[3]Department of Structural Analysis, National Cardiovascular Center Research Institute, Osaka 565-8565, Japan

The cardiac homeobox transcription factor CSX/NKX2-5 plays an important role in vertebrate heart development. Using a yeast two-hybrid screening, we identified a novel LIM domain–containing protein, named CSX-associated LIM protein (Cal), that interacts with CSX/NKX2-5. CSX/NKX2-5 and Cal associate with each other both in vivo and in vitro, and the LIM domains of Cal and the homeodomain of CSX/NKX2-5 were necessary for mutual binding. Cal itself possessed the transcription-promoting activity, and cotransfection of Cal enhanced CSX/NKX2-5–induced activation of *atrial natriuretic peptide* gene promoter. Cal contained a functional nuclear export signal and shuttled from the cytoplasm into the nucleus in response to calcium. Accumulation of Cal in the nucleus of P19CL6 cells promoted myocardial cell differentiation accompanied by increased expression levels of the target genes of CSX/NKX2-5. These results suggest that a novel LIM protein Cal induces cardiomyocyte differentiation through its dynamic intracellular shuttling and association with CSX/NKX2-5.

Introduction

CSX/NKX2-5 is a member of NK homeobox gene family that is conserved in evolution and acts as a DNA-binding transcription activator (Komuro and Izumo, 1993; Lints et al., 1993; Akazawa and Komuro, 2003). During embryogenesis, *CSX/NKX2-5* is expressed predominantly in the heart progenitor cells from the very early stage. Targeted disruption of murine *CSX/NKX2-5* resulted in embryonic lethality due to the arrested looping morphogenesis of the heart tube (Lyons et al., 1995). In addition, mutations of *CSX/NKX2-5* cause human hereditary cardiac malformations associated with atrioventricular conduction disturbance (Schott et al., 1998). These results indicate that *CSX/NKX2-5* plays a pivotal role in normal heart development in mammals.

To understand the mechanisms of how *CSX/NKX2-5* controls cardiac development, it is necessary to elucidate the molecular framework of fine-tuned transcriptional regulation of its distinct target genes. Recently, protein–protein interactions have been recognized to be important in many biological processes. Protein complexes consisting of transcription factors and cofactors are responsible for transcriptional regulation, and its composition is thought to be the key determinant of specificity and intensity of the reaction. Transcriptional activity of CSX/NKX2-5 is modulated through physical interaction with other transcription factors such as GATA-4 (Durocher et al., 1997; Lee et al., 1998; Shiojima et al., 1999), SRF (Chen and Schwartz, 1996), and Tbx-5 (Bruneau et al., 2001; Hiroi et al., 2001). Here, we isolated a novel CSX/NKX2-5–associated protein by a yeast two-hybrid screening using *CSX/NKX2-5* as a bait. The protein was a novel LIM domain–containing protein, which we named CSX-associated LIM protein (*Cal*). The LIM domain is a double-zinc finger motif and functions as a module for protein–protein interactions (Dawid et al., 1998; Bach, 2000). Nuclear LIM proteins such as LIM homeodomain proteins and LIM only proteins are directly involved in transcriptional regulation during cell differentiation (Dawid et al., 1998; Bach, 2000). Cytoplasmic LIM proteins are involved in divergent biological processes such as regulation of cytoarchitecture, protein trafficking, and specification of cell polarity (Dawid et al., 1998; Bach,

Address correspondence to Issei Komuro, Dept. of Cardiovascular Science and Medicine, Chiba University Graduate School of Medicine, 1-8-1 Inohana, Chuo-ku, Chiba 260-8670, Japan. Tel.: 81-43-226-2097. Fax: 81-43-226-2557. email: komuro-tky@umin.ac.jp

Key words: cardiogenesis; homeobox transcription factor; LIM domain; nucleocytoplasmic transport; transcriptional regulation

Abbreviations used in this paper: ANP, atrial natriuretic peptide; Ca^{2+}, calcium; Cal, CSX-associated LIM protein; CRP, cysteine-rich protein; LMB, leptomycin B; LPP, lipoma preferred partner; NES, nuclear export signal; SERCA2, sarcoplasmic reticulum Ca^{2+}-ATPase 2; trip6, thyroid receptor interacting protein 6.

The Journal of Cell Biology, Volume 164, Number 3, February 2, 2004 395–405
http://www.jcb.org/cgi/doi/10.1083/jcb.200309159

2000). In regard to muscle development, the roles of cysteine-rich protein (CRP) 3/MLP, which is primarily cytoplasmic, have attracted much attention (Arber et al., 1994). Overexpression of CRP3/MLP in C2C12 myoblasts promoted skeletal myogenesis, whereas inhibition of CRP3/MLP activity by antisense oligonucleotide interrupted terminal differentiation of these cells. Mice homozygous for CRP3/MLP mutation exhibited dilated cardiomyopathy resulted from disrupted cytoarchitecture in cardiomyocytes (Arber et al., 1997). These results indicate the possibility that cytoplasmic LIM proteins regulate cell differentiation as well. Recently, some cytoplasmic LIM proteins have been reported to show nuclear localization. For example, CRP3/MLP associates with nuclear LIM proteins Lmo1 and Apterous (Arber and Caroni, 1996) and basic helix-loop-helix transcription factor MyoD (Kong et al., 1997) as well as cytoskeletal proteins, Zyxin, and α actinin (Louis et al., 1997). However, the molecular mechanism by which the cytoplasmic LIM proteins are involved in nuclear events remains largely unknown.

Here, we show that Cal functions as a coactivator for CSX/NKX2-5 and fulfills its cooperative function based on its dynamic intracellular shuttling mechanisms. Consistent with the notion that the LIM domains function as an interface of protein–protein interactions, the LIM domains of Cal are required for binding to the homeodomain of CSX/NKX2-5. Cal itself has the transcription-promoting activity and activates the *atrial natriuretic peptide* (*ANP*) promoter by forming complex with CSX/NKX2-5. Cal traffics out of the nucleus by nuclear export signal (NES)–dependent mechanisms and traffics into the nucleus in response to an increase of intracellular calcium (Ca^{2+}) concentration. Nuclear expression of Cal promotes cardiac differentiation of P19CL6 cells in vitro. Characterization of complex formation between CSX/NKX2-5 and Cal will provide a unique framework whereby gene expression during cardiogenesis is fine-tuned by the primarily cytoplasmic LIM proteins that were supposed to be involved in cytoskeletal organization.

Results

Molecular cloning and characterization of Cal

To identify proteins that interact with CSX/NKX2-5, we screened a human heart library by the yeast two-hybrid system using the full length of *CSX/NKX2-5* as a bait, and isolated a gene out of 25 positive clones, which we named *Cal*. Using the human Cal cDNA, we isolated the mouse full-length *Cal* cDNA, which encodes a protein of 375 aa (Fig. 1 A) with three tandemly arrayed LIM domains in the COOH terminus. It contains a region abundant in proline residues in the NH_2 terminus. In addition, there is a leucine-rich motif that matches the consensus sequence for NES. These salient structural features are shared among Zyxin family of LIM domain–containing proteins consisting of *Zyxin* (Beckerle, 1997), *lipoma preferred partner* (*LPP*) (Petit et al., 1996), *Ajuba* (Goyal et al., 1999), and *thyroid receptor interacting protein 6 (trip6;* Yi and Beckerle, 1998). Northern blot analysis revealed that there were two transcripts of different sizes, 3.2 and 6.0 kb, and that Cal was highly expressed in a variety of tissues (Fig. 1 B). Most abundant expression was observed in the heart and relatively abundant expression was observed in the lung, intestine, and uterus, whereas little transcript was detected in the brain and liver. RNA in situ hybridization studies revealed that *Cal* was ex-

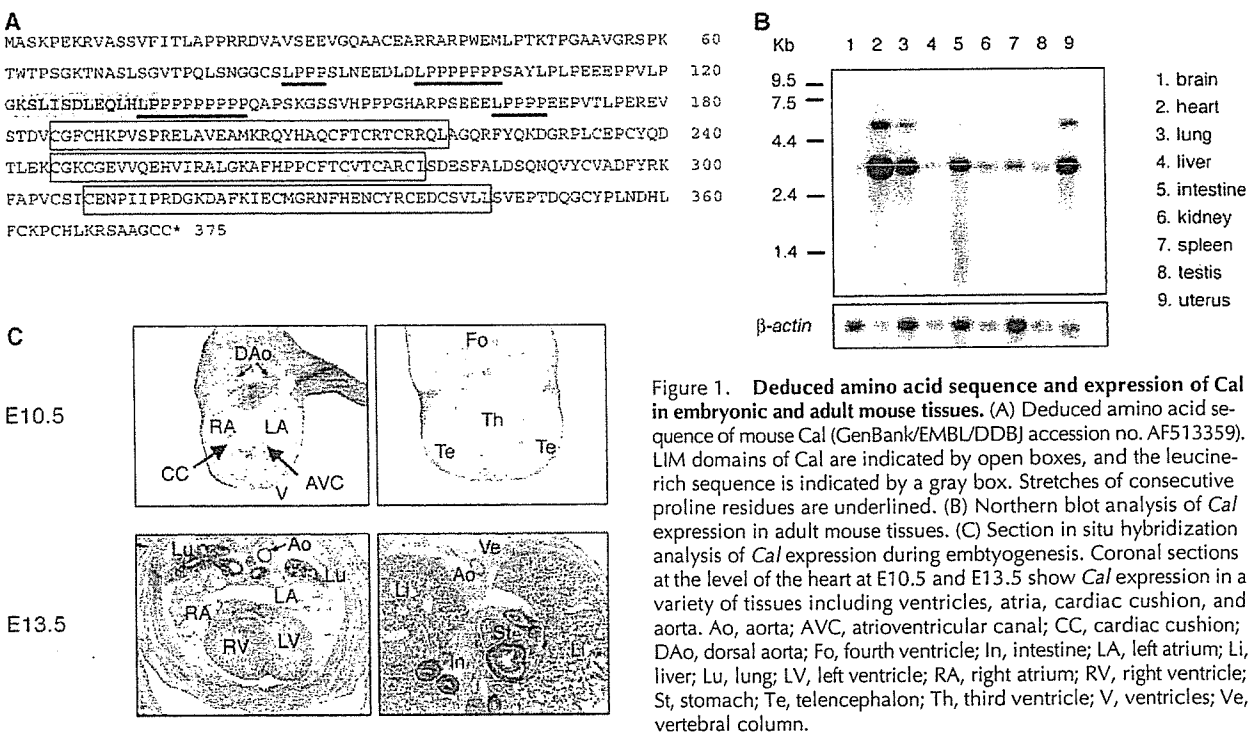

Figure 1. **Deduced amino acid sequence and expression of Cal in embryonic and adult mouse tissues.** (A) Deduced amino acid sequence of mouse Cal (GenBank/EMBL/DDBJ accession no. AF513359). LIM domains of Cal are indicated by open boxes, and the leucine-rich sequence is indicated by a gray box. Stretches of consecutive proline residues are underlined. (B) Northern blot analysis of *Cal* expression in adult mouse tissues. (C) Section in situ hybridization analysis of *Cal* expression during embtyogenesis. Coronal sections at the level of the heart at E10.5 and E13.5 show *Cal* expression in a variety of tissues including ventricles, atria, cardiac cushion, and aorta. Ao, aorta; AVC, atrioventricular canal; CC, cardiac cushion; DAo, dorsal aorta; Fo, fourth ventricle; In, intestine; LA, left atrium; Li, liver; Lu, lung; LV, left ventricle; RA, right atrium; RV, right ventricle; St, stomach; Te, telencephalon; Th, third ventricle; V, ventricles; Ve, vertebral column.

pressed in a wide variety of cell-lineages including the heart, lung, and intestine during mouse embryogenesis (Fig. 1 C). Lesser transcript was observed in the liver, and no transcript was observed in the vertebral column and encephalon.

Cal forms a complex with CSX/NKX2-5

To examine whether CSX/NKX2-5 and Cal directly interact with each other in vivo, we cotransfected COS7 cells with HA-tagged CSX/NKX2-5 and FLAG-tagged Cal. Cell lysates were subjected to immunoprecipitation using anti-FLAG antibody, and coprecipitating CSX/NKX2-5 was detected by immunoblotting with anti-HA antibody (Fig. 2 A). This result suggests that CSX/NKX2-5 and Cal associate with each other in mammalian cells as well as yeast cells.

Next, to confirm the direct interaction between CSX/NKX2-5 and Cal, and if so, to determine the domain responsible for the association, GST pull-down assays were performed with GST-Cal fusion protein and in vitro–translated CSX/NKX2-5. GST-Cal immobilized on glutathione-Sepharose beads retained in vitro–translated CSX/NKX2-5, indicating the direct interaction between CSX/NKX2-5 and Cal (Fig. 2 B). A CSX/NKX2-5 mutant lacking the homeodomain did not associate with Cal, but the homeodomain of CSX/NKX2-5 was enough for association (Fig. 2 B). These results suggest that the homeodomain of CSX/NKX2-5 is necessary and sufficient for the interaction with Cal. We also examined the binding of GST-CSX/NKX2-5 and in vitro–translated Cal and its mutants. A Cal mutant lacking all three LIM domains did not associate with CSX/NKX2-5, but Cal mutants containing at least two LIM domains did associate with CSX/NKX2-5 (Fig. 2 C). These results suggest that the LIM domains of Cal are responsible for interaction with CSX/NKX2-5.

CSX/NKX2-5 and Cal synergistically transactivate the ANP promoter

To examine the effect of Cal on transcriptional activity of CSX/NKX2-5, we performed a series of reporter assays using the luciferase reporter linked to the *ANP* promoter. When the luciferase construct containing the *ANP* promoter was cotransfected with CSX/NKX2-5 expression vector, significant fold induction of the promoter activity was observed as reported previously (Shiojima et al., 1999). Although overexpression of Cal had no effect on the *ANP* promoter, cotransfection of Cal with CSX/NKX2-5 induced much stronger transactivation than CSX/NKX2-5 alone, suggesting that CSX/NKX2-5 and Cal synergistically transactivate the *ANP* promoter (Fig. 3 A). CSX/NKX2-5 and Cal also synergistically transactivated the luciferase construct containing multimerized CSX/NKX2-5–binding sites (Fig. 3 A).

Next, we examined whether the interaction between CSX/NKX2-5 and Cal was required for the synergistic

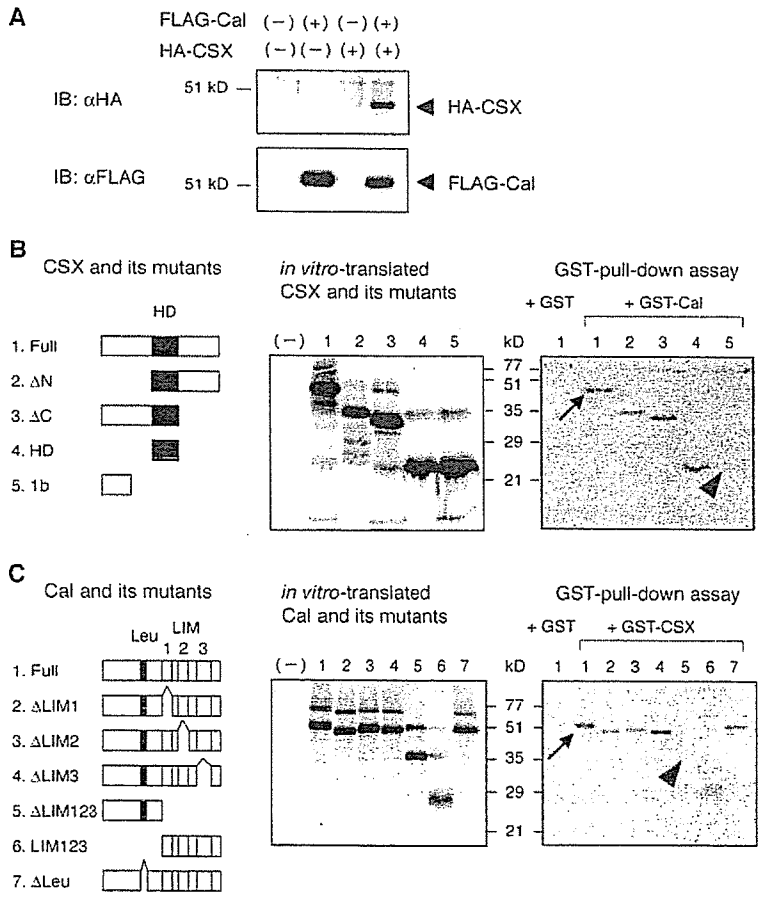

Figure 2. **Complex formation between CSX/NKX2-5 and Cal.** (A) Coimmunoprecipitation of CSX/NKX2-5 and Cal in transfected COS7 cells. Immunoprecipitates with anti-FLAG antibody were separated by SDS-PAGE and immunoblotted with anti-HA antibody (top). The same blot was reprobed with anti-FLAG antibody to confirm the presence of FLAG-tagged Cal (bottom). (B) GST pull-down assay for mapping of a region in CSX/NKX2-5 required for binding to Cal. In vitro–translated CSX/NKX2-5 and its mutants labeled with ^{35}S were incubated with GST-Cal immobilized on glutathione-Sepharose beads, and bound proteins were separated by SDS-PAGE and visualized by autoradiography. The arrow indicates the CSX/NKX2-5 protein bound to GST-Cal. A CSX/NKX2-5 mutant lacking the homeodomain did not associate with Cal (arrowhead), whereas a CSX/NKX2-5 mutant containing only the homeodomain did associate. HD, homeodomain. (C) GST pull-down assay for mapping of a region in Cal required for binding to CSX/NKX2-5. In vitro–translated Cal and its mutants labeled with ^{35}S were incubated with GST-CSX/NKX2-5. The arrow indicates the Cal protein bound to GST-CSX/NKX2-5. A Cal mutant lacking all the LIM domains did not associate with CSX/NKX2-5 (arrowhead), whereas a Cal mutant containing only the LIM domains did associate.

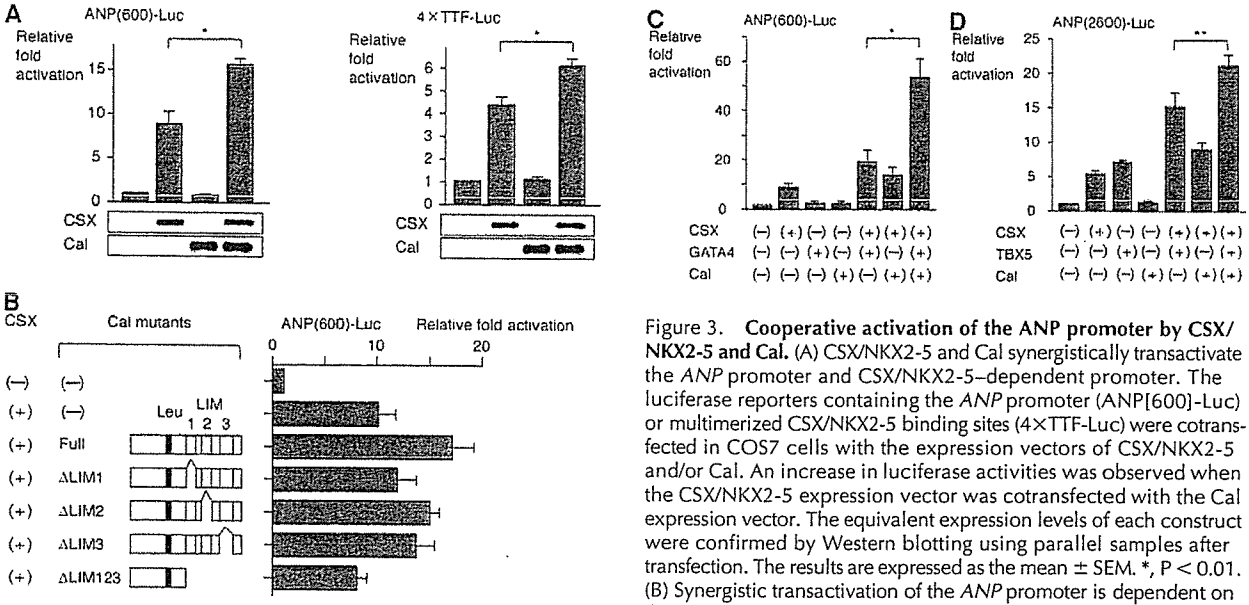

Figure 3. **Cooperative activation of the ANP promoter by CSX/NKX2-5 and Cal.** (A) CSX/NKX2-5 and Cal synergistically transactivate the *ANP* promoter and CSX/NKX2-5–dependent promoter. The luciferase reporters containing the *ANP* promoter (ANP[600]-Luc) or multimerized CSX/NKX2-5 binding sites (4×TTF-Luc) were cotransfected in COS7 cells with the expression vectors of CSX/NKX2-5 and/or Cal. An increase in luciferase activities was observed when the CSX/NKX2-5 expression vector was cotransfected with the Cal expression vector. The equivalent expression levels of each construct were confirmed by Western blotting using parallel samples after transfection. The results are expressed as the mean ± SEM. *, $P < 0.01$. (B) Synergistic transactivation of the *ANP* promoter is dependent on the interaction between CSX/NKX2-5 and Cal. A Cal mutant lacking all three LIM domains, the docking module for binding to CSX/NKX2-5, exhibited no significant cooperation on CSX/NKX2-5–induced promoter activation. The results are expressed as the mean ± SEM. (C) Cal augments synergistic transactivation between CSX/NKX2-5 and GATA-4. COS7 cells were cotransfected with the luciferase reporter containing the *ANP* promoter (ANP[600]-Luc) and the expression vectors of CSX/NKX2-5 and/or GATA-4 and/or Cal. Cotransfection with CSX/NKX2-5 and GATA-4 exhibited synergistic transactivation, that was further enhanced by additional expression of Cal. The results are expressed as the mean ± SEM. *, $P < 0.01$. (D) Cal augments synergistic transactivation between CSX/NKX2-5 and Tbx-5. Cotransfection with CSX/NKX2-5 and Tbx-5 exhibited synergistic transactivation of the *ANP* promoter (ANP[2600]-Luc), that was further augmented by additional expression of Cal. The results are expressed as the mean ± SEM. **, $P < 0.05$.

transactivation of the *ANP* promoter. Although Cal mutants lacking one LIM domain, which retain the ability to bind to CSX/NKX2-5, showed synergistic activation with CSX/NKX2-5 on the *ANP* promoter, the Cal mutant lacking the three LIM domains, which does not bind to CSX/NKX2-5, exhibited no significant cooperation on CSX/NKX2-5–induced promoter activation (Fig. 3 B). These results suggest that the synergistic transactivation was dependent on the mutual binding between CSX/NKX2-5 and Cal.

It has been reported that CSX/NKX2-5 and a zinc-finger transcription factor, GATA-4, display synergistic transcriptional activation of the *ANP* promoter (Durocher et al., 1997; Lee et al., 1998; Shiojima et al., 1999). As shown in Fig. 3 C, Cal augmented this synergistic promoter activation between CSX/NKX2-5 and GATA4. We and others reported recently that CSX/NKX2-5 and a T-box transcription factor, Tbx-5, showed synergistic transcriptional activation of the *ANP* promoter (Bruneau et al., 2001; Hiroi et al., 2001). Cal also augmented this synergistic promoter activation between CSX/NKX2-5 and Tbx-5 (Fig. 3 D).

Cal is a transactivator

To understand how Cal exhibits synergistic transcriptional activation with CSX/NKX2-5, we examined the transcriptional activity of Cal. The expression vector containing Cal fused to GAL4 DNA-binding domain was cotransfected in COS7 cells with the luciferase reporter containing the multimerized GAL4-binding sites. As shown Fig. 4, full length of Cal fused to the DNA-binding domain of GAL4 transactivated a GAL4-dependent reporter ~13.0-fold compared with DNA-binding domain of GAL4 alone. Cal mutants lacking all three LIM domains, LIM2 or LIM3 domains showed no transcriptional activity, whereas the Cal mutant containing only LIM2 and LIM3 domains showed stronger activity than the full length of Cal. Deletion of LIM1 domain showed even stronger activity, suggesting that Cal itself has the transcription-promoting activity and that its transactivation domain is localized

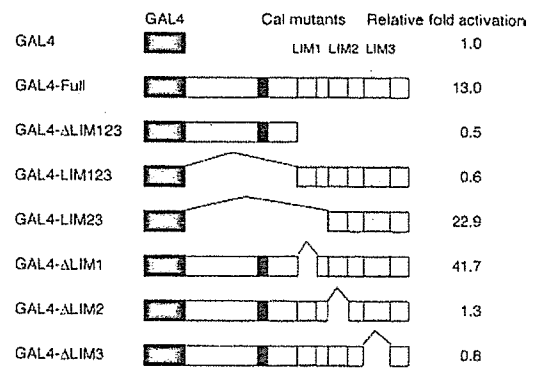

Figure 4. **Transcriptional activity of Cal.** Expression vectors encoding the GAL4 DNA binding domain fused to the indicated regions of Cal were transiently transfected into COS7 cells with the pG5luc-luciferase reporter, which contained five GAL4 binding sites. Cal fused to the DNA binding domain of GAL4 significantly transactivated a GAL4-dependent reporter, indicating that Cal possesses transcriptional activity. Cal mutants lacking LIM2 or LIM3 showed no transcriptional activity, whereas Cal mutants containing LIM2 and LIM3 showed stronger activity.

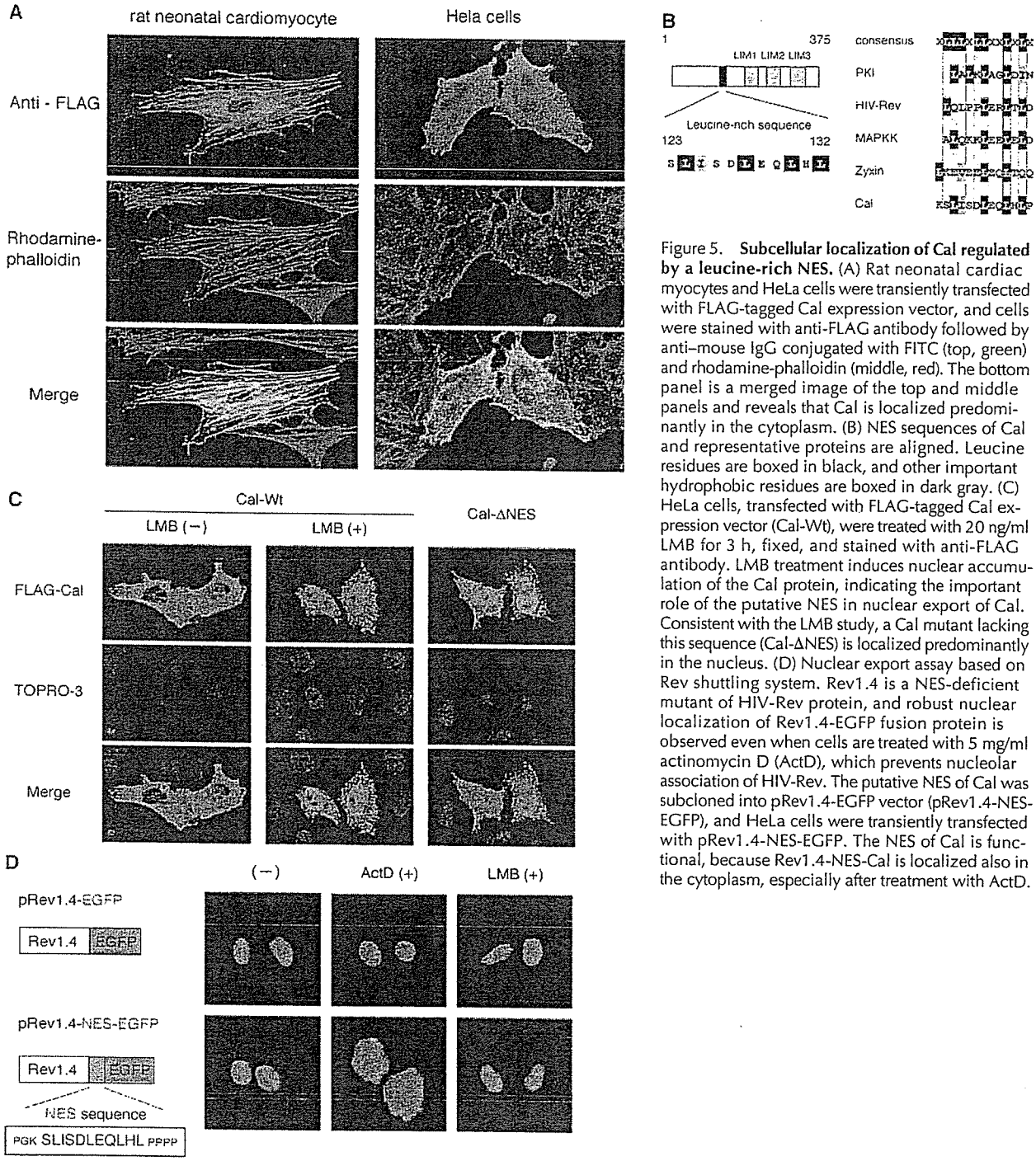

Figure 5. **Subcellular localization of Cal regulated by a leucine-rich NES.** (A) Rat neonatal cardiac myocytes and HeLa cells were transiently transfected with FLAG-tagged Cal expression vector, and cells were stained with anti-FLAG antibody followed by anti–mouse IgG conjugated with FITC (top, green) and rhodamine-phalloidin (middle, red). The bottom panel is a merged image of the top and middle panels and reveals that Cal is localized predominantly in the cytoplasm. (B) NES sequences of Cal and representative proteins are aligned. Leucine residues are boxed in black, and other important hydrophobic residues are boxed in dark gray. (C) HeLa cells, transfected with FLAG-tagged Cal expression vector (Cal-Wt), were treated with 20 ng/ml LMB for 3 h, fixed, and stained with anti-FLAG antibody. LMB treatment induces nuclear accumulation of the Cal protein, indicating the important role of the putative NES in nuclear export of Cal. Consistent with the LMB study, a Cal mutant lacking this sequence (Cal-ΔNES) is localized predominantly in the nucleus. (D) Nuclear export assay based on Rev shuttling system. Rev1.4 is a NES-deficient mutant of HIV-Rev protein, and robust nuclear localization of Rev1.4-EGFP fusion protein is observed even when cells are treated with 5 mg/ml actinomycin D (ActD), which prevents nucleolar association of HIV-Rev. The putative NES of Cal was subcloned into pRev1.4-EGFP vector (pRev1.4-NES-EGFP), and HeLa cells were transiently transfected with pRev1.4-NES-EGFP. The NES of Cal is functional, because Rev1.4-NES-Cal is localized also in the cytoplasm, especially after treatment with ActD.

within the LIM2 and LIM3 domains, whereas LIM1 may function as a repressor domain.

Cal is predominantly localized in the cytoplasm and shuttles between the cytoplasm and the nucleus

We examined the subcellular localization of Cal protein in cultured cells. Cultured cardiac myocytes of neonatal rats were transiently transfected with FLAG-tagged Cal expression vector, and immunofluorescence analysis was performed using anti-FLAG antibody. Cal protein was predominantly localized in the cytoplasm of cardiac myocytes at steady state (Fig. 5 A). Similar pattern of immunofluorescence was obtained in other cell lines such as HeLa (Fig. 5 A), COS7, and NIH3T3 cells (not depicted).

Within the amino acid sequence of Cal, there was a leucine-rich sequence that matched the consensus sequence of NES (Fig. 5 B). During a nuclear export cycle, an exportin molecule CRM1 recognizes the NES and forms a complex

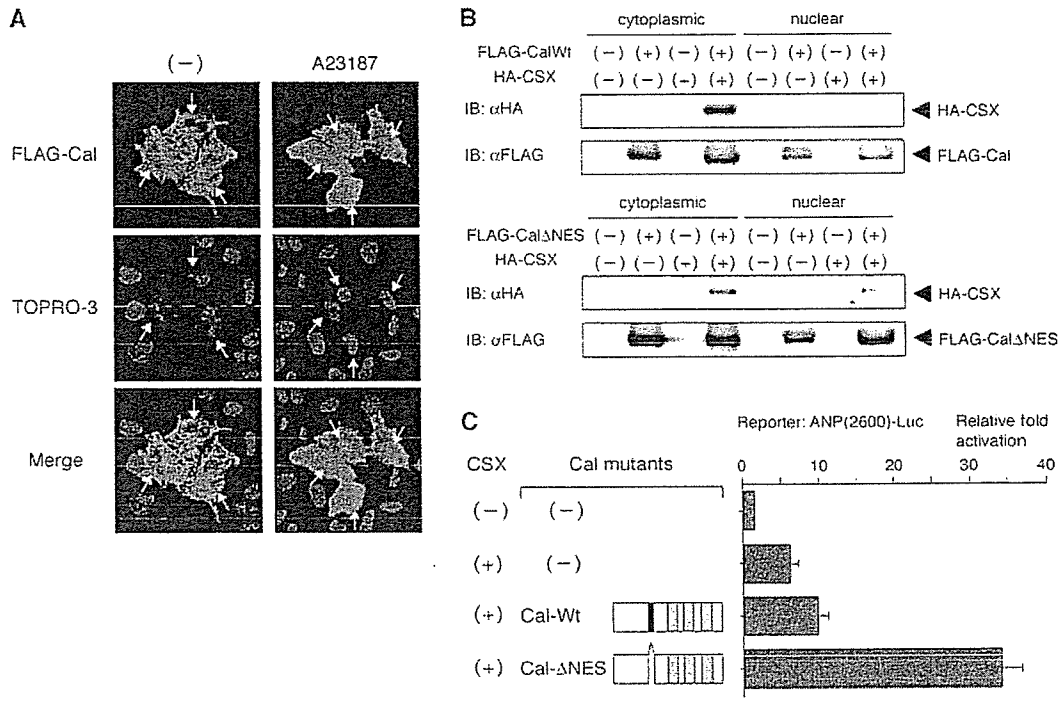

Figure 6. **Nuclear transport of Cal in response to calcium ionophore and implications of nuclear accumulation of Cal in transcriptional cooperativity with CSX/NKX2-5.** (A) HeLa cells, transfected with FLAG-tagged Cal expression vector, were treated with vehicle or calcium ionophore A23187 (2 μM) for 15 min, fixed, and stained with anti-FLAG antibody. Nuclear accumulation of Cal is observed in significant portions of transfected cells after treatment with A23187. The arrows indicate the nuclei of the transfected cells. (B) Coimmunoprecipitation of CSX/NKX2-5 and Cal (Cal-Wt) or nuclear form of Cal (Cal-ΔNES) in preparations of cytoplasmic or nuclear fractions of transfected COS7 cells. Cal-ΔNES showed significantly stronger interaction with CSX/NKX2-5 in the nucleus than Cal-Wt. (C) The luciferase reporter containing the *ANP* promoter was cotransfected in COS7 cells with the expression vectors of CSX/NKX2-5 and Cal-Wt or Cal-ΔNES. Cal-ΔNES showed much stronger synergistic activation with CSX/NKX2-5 than Cal-Wt. The results are expressed as the mean ± SEM.

with RanGTP, and mediates transport to the cytoplasm (Fornerod et al., 1997; Mattaj and Englmeier, 1998; Ohno et al., 1998; Kuersten et al., 2001). NES-dependent nuclear export is inhibited by leptomycin B (LMB) that interferes with the binding of CRM1 to NES (Kudo et al., 1998). Inhibition of CRM1-dependent nuclear export using LMB resulted in rapid nuclear accumulation of Cal protein in HeLa cells (Fig. 5 C). Although immunofluorescence studies indicated that the main compartment where Cal is localized at steady state was the cytoplasm, the accumulation of CAL after treatment with LMB suggested that Cal can shuttle between the cytoplasm and the nucleus.

To confirm that the putative NES contributes to nuclear export of Cal, we deleted the NES sequence (residues 123–132) in the FLAG-tagged Cal expression vector (Cal-ΔNES) and examined the subcellular localization of Cal-ΔNES mutant. Cal-ΔNES was predominantly localized in the nucleus (Fig. 5 C), suggesting that this sequence mediates the CRM1-dependent nuclear export of Cal. To test this sequence of Cal functions as an NES, we introduced this sequence into the export-deficient form of Rev-EGFP, and tested its nuclear export activity in HeLa cells. The putative NES of Cal displayed the export activity, especially in the presence of actinomycin D, which prevents nucleolar association of Rev protein (Fig. 5 D). These results indicate that this 123-132–amino acid sequence of Cal really functions as an NES.

Cal shuttles into the nucleus in response to Ca^{2+} signal

We explored a specific signal capable of targeting Cal protein to the nucleus. When intracellular Ca^{2+} levels were increased by Ca^{2+} ionophore A23187, Cal protein was transported to the nucleus (Fig. 6 A). Nuclear accumulation of Cal was detected at 10 min after addition of A23187. No other cellular signals possessed ability to transport Cal into the nucleus. For example, treatment with cytochalasin D, an actin filament disrupting reagent, tetradecanoylphorbol 13-acetate, PKC activator, forskolin, an adenylate cyclase activator, anisomycin, Jun-NH_2–terminal kinase agonist, okadaic acid, a serine/threonine phosphatase inhibitor did not induce nuclear translocation of Cal protein.

Next, we examined whether nucleocytoplasmic shuttling of Cal protein had important implications for modifying the transcriptional activity of CSX/NKX2-5. As indicated by coimmunoprecipitation experiments by using cytoplasmic and nuclear fractions of transfected cells, interaction between CSX/NKX2-5 and wild-type of Cal (Cal-Wt) was detectable predominantly in the cytoplasm and slightly in the nucleus (Fig. 6 B). When Cal-ΔNES, which lacks the NES and is predominantly localized in the nucleus, was cotransfected, the level of coprecipitating CSX/NKX2-5 in the nuclear fraction increased significantly (Fig. 6 B). Furthermore, Cal-ΔNES showed much stronger synergistic transactivation of the *ANP* promoter than Cal-Wt, when cotransfected with CSX/

NKX2-5 (Fig. 6 C). These results suggest that nuclear translocation of Cal enhances CSX/NKX2-5–induced promoter activation by promoting mutual interaction in the nucleus.

Nuclear accumulation of Cal induces cardiac differentiation of P19CL6 cells

To determine whether synergistic transactivation by Cal has a significant effect on cardiomyocyte differentiation, we isolated P19CL6 clones, which stably overexpress wild-type Cal (P19CL6-CAL-Wt) or Cal mutant lacking the NES (P19CL6-Cal-ΔNES). When cultured in the medium containing 1% DMSO, P19CL6 cells differentiated into cardiomyocytes, which exhibit spontaneous beating and express cardiac-specific genes (Monzen et al., 1999). The expression of cardiac-specific genes was examined in P19CL6 cells, P19CL6-Cal-Wt, and P19CL6-Cal-ΔNES during differentiation (Fig. 7 A). Northern blot analysis revealed that expression levels of a cardiac transcription factor *GATA-4* and *sarcoplasmic reticulum Ca^{2+}-ATPase 2* (*SERCA2*) as well as *connexin 43* and *calreticulin*, known as downstream targets for CSX/NKX2-5, were increased in P19CL6-Cal-ΔNES cells. RT-PCR analysis revealed that expression of *ANP* gene was also up-regulated in P19CL6-Cal-ΔNES cells, which was consistent with the results that Cal augmented *ANP* promoter activation induced by CSX/NKX2-5. Immunocytochemical analysis revealed that in P19CL6-Cal-ΔNES, a larger number of cells were stained positive with anticardiac troponin T antibody than the parental P19CL6 cells (Fig. 7 B), suggesting that nuclear accumulation of Cal strongly promotes cardiac differentiation.

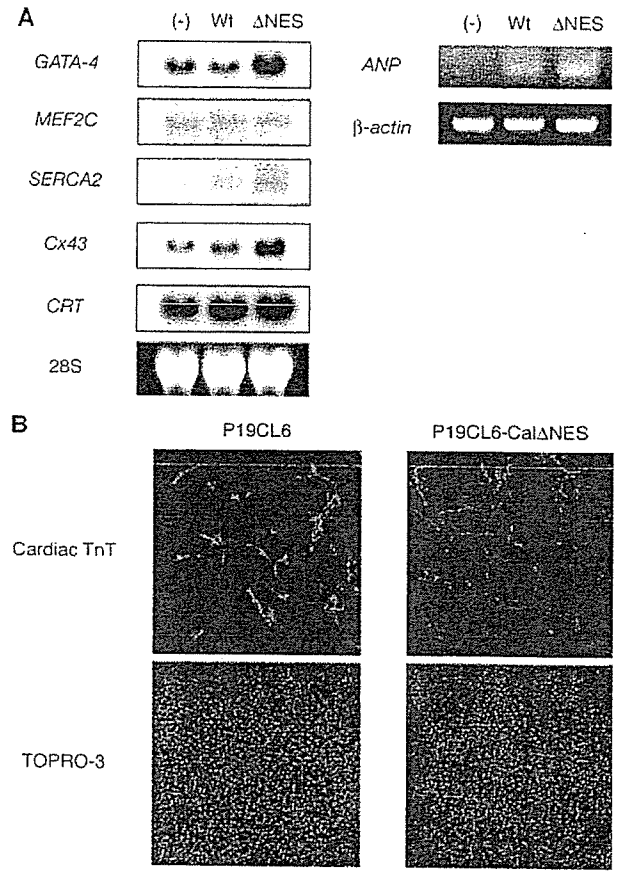

Figure 7. **Promotion of cardiac differentiation in P19CL6 cells by nuclear accumulation of Cal.** (A) Expression of cardiac genes was examined on differentiation day nine of P19CL6 cells, P19CL6 cells stably expressing Cal-Wt and Cal-ΔNES. Northern blot analysis was performed with *GATA-4, MEF2C, SERCA2, Connexin43* (*Cx43*), and *calreticulin* (*CRT*) cDNAs and RT-PCR was performed using specific primers for *ANP*. Notably, expression levels of target genes for CSX/NKX2-5 such as *Cx43, CRT,* and *ANP* were increased in P19CL6-Cal-ΔNES. (B) Cardiac differentiation in P19CL6 cells on differentiation day 14 was determined by immunofluorescence with anticardiac troponin T (TnT) antibody. Much larger number of cells were stained positive for cardiac TnT in P19CL6-Cal-ΔNES.

Discussion

Cal is a novel LIM domain–containing protein

We identified a novel protein Cal, which associates with the cardiac homeobox transcription factor CSX/NKX2-5. *Cal* is a member of Zyxin family, that commonly have a proline-rich region at the NH_2 terminus, a leucine-rich sequence, and three tandem LIM domains located at the COOH terminus. The proline-rich regions of Zyxin serve as interface to bind to SH3 domain of Vav (Hobert et al., 1996) and EVH1 domain of Ena/VASP family proteins (Renfranz and Beckerle, 2002) that are implicated in control of actin organization (Gertler et al., 1996). LPP also contains proline-rich motifs that are required for the interaction with the EVH1 domain (Prehoda et al., 1999). This proline-rich region of LPP directly interacts with VASP in vitro, and LPP is colocalized with VASP in the focal adhesion. The proline-rich regions of Ajuba interact with Grb2 (Goyal et al., 1999). Expression of Ajuba enhances MAPK activity in fibroblasts and promotes meiotic maturation of *Xenopus* oocytes through activation of MAPK in Grb2- and Ras-dependent manner (Goyal et al., 1999). The NH_2-terminal portion of *Cal* also contains stretches of proline-rich sequences. Especially, two proline-rich sequences (LPPPPPPP 98-105 and LPPPPPPPPP 133-142) of Cal lead us to speculate that Cal might associate with profilin and be involved in the organization of cytoskeletal actin in the cytoplasm because the sequence of consecutive prolines flanked by leucine has been thought to be a ligand motif for profilin (Mahoney et al., 1997). Identification of proteins binding to the proline-rich region of Cal would provide further insights into its cellular function.

Cal interacts with CSX/NKX-2.5 both in vitro and in vivo

GST pull-down assays and coimmunoprecipitation experiments indicated the association of Cal with CSX/NKX2-5 both in vitro and in vivo. Analyses using mutants of both proteins revealed that the mutual binding was mediated through the homeodomain of CSX/NKX2-5 and the LIM domains of Cal. Besides binding to DNA, the homeodomain of CSX/NKX2-5 acts as a module for the interaction with its binding partner such as GATA-4 (Durocher et al., 1997; Lee et al., 1998; Shiojima et al., 1999), SRF (Chen and Schwartz, 1996), and Tbx-5 (Hiroi et al., 2001). The LIM domains of Cal have a cysteine-histidine rich, double zinc-finger motif that functions as a protein–protein in-

teraction module (Dawid et al., 1998; Bach, 2000). The LIM domains of Zyxin interact with members of CRP family (Sadler et al., 1992) and serine/threonine kinase h-warts/LATS1 (Hirota et al., 2000). During mitosis, phosphorylation of Zyxin by Cdc2 promotes the binding between Zyxin and h-warts/LATS1, and the complex is targeted to the mitotic apparatus. The possibility that interaction between CSX/NKX2-5 and Cal is modulated by specific protein modification remains to be determined.

Abundant expression of *Cal* was detected in the heart during embryogenesis and maintained in the atrial and ventricular chambers through the adulthood. *Cal* was also expressed in a variety of tissues such as the aorta, lung, and intestine, but little expression was detected in the brain and liver. Although the functional roles of Cal in tissues other than the heart remain unknown at present, Cal may associate with other NK homeobox transcription factors, because the amino acid sequences of homeodomains, which are responsible for binding to Cal, are highly conserved among this class of homeoproteins. Interestingly, Ajuba has been reported to associate with thyroid transcription factor-1/Nkx2-1, a member of NK homeobox transcription factors, in mammalian cells, although the physiological function of their interaction remains unknown (Missero et al., 2001). It is possible that there are more combinatorial patterns of physical interaction between Zyxin family LIM proteins and NK homeoproteins.

Cal shuttles between the cytoplasm and the nucleus

The leucine-rich sequence of Cal is thought to function as an NES, based on the following results: (a) the leucine-rich sequence of Cal matches the consensus of the NES; (b) predominant nuclear distribution was observed when treated with LMB, that is a specific inhibitor of CRM1-dependent nuclear export (Kudo et al., 1998); (c) the Cal mutant lacking the leucine-rich sequence was localized predominantly in the nucleus; and (d) fusion of leucine-rich sequence of Cal to Rev1.4-EGFP transported the Rev1.4-EGFP from the nucleus to the cytoplasm (Henderson, 2000). Functional leucine-rich NESs have been identified in other Zyxin family members such as *Zyxin* (Nix and Beckerle, 1997), *trip6* (Wang and Gilmore, 2001), *LPP* (Petit et al., 2000), and *Ajuba* (Kanungo et al., 2000). Although the role of Zyxin family members in the nucleus has not been fully defined, the interaction between Zyxin and h-wartz/LATS1 on the mitotic apparatus implicates the specific role of Zyxin in the regulation of cell cycle (Hirota et al., 2000).

Cal augments CSX/NKX2-5–induced promoter activation

The interaction between CSX/NKX2-5 and Cal implicates a certain role of transcriptional regulation of cardiac-specific genes. CSX/NKX2-5 and Cal synergistically activated both the *ANP* promoter and the artificial promoter containing multimerized CSX/NKX2-5–binding sites. Furthermore, Cal enhanced cooperative promoter activation of *ANP* gene between CSX/NKX2-5 and GATA-4 or Tbx-5. These results suggest that transcriptional regulation by cardiac transcription factors may be fulfilled harmoniously by multiprotein complex.

The GAL4-based reporter assay revealed that Cal itself possesses transcriptional activity. LIM2 and LIM3 domains were endowed with the capacity to activate transcription, whereas the LIM1 domain suppressed the transcriptional activity. On the other hand, the ΔLIM1 mutant failed to augment CSX/NKX2-5–induced transactivation of the *ANP* reporter (Fig. 3 B). GST pull-down assays revealed that the LIM domains are required for binding to CSX/NKX2-5 and that deletion of LIM1 reduced the mutual binding (Fig. 2 C), suggesting that deletion of LIM1 may also decrease the binding affinity for CSX/NKX2-5. In addition, there is a possibility that the LIM1 interferes the GAL4-DNA binding but not inhibits the transcription. It has been reported that Trip6 and LPP have transcriptional activity, and the transactivation domains were attributed to the LIM domains and a region containing the NES of *trip6* (Wang and Gilmore, 2001) and to the LIM domains and the proline-rich region of *LPP* (Kanungo et al., 2000). Based on the fact that transactivation domains reside in modules for protein–protein interaction, it is likely that the interaction with components of transcriptional initiation complex is involved in transcriptional activation.

Cooperative transactivation of the *ANP* promoter by CSX/NKX2-5 and Cal was enhanced when Cal protein was targeted into the nucleus by deleting its NES. We found that treatment with Ca^{2+} ionophore A23187 induced nuclear transport of Cal. Pathophysiological significance of Ca^{2+} signaling in cardiac development has not been fully defined. However, Ca^{2+} signals are induced by various conditions including G-protein–coupled receptors (Clapham, 1995) and receptor tyrosine kinases (Schlessinger, 2000). It is possible to assume that Cal might modulate the transcriptional activity of CSX/NKX2-5 in response to Ca^{2+} signals triggered by G-protein–coupled receptors or receptor tyrosine kinases during cardiogenesis. Exploration of physiological ligands that activate Ca^{2+} signals and subsequent nuclear import of Cal will undermine the molecular framework of cardiac development.

Ca^{2+} signaling plays an important role in generation of cardiac hypertrophy (Frey et al., 2000). Nuclear import of NF-AT transcription factors is induced by Ca^{2+}-activated phosphatase calcineurin and that transgenic mice expressing nuclear form of NF-AT3 in the heart exhibited cardiac hypertrophy (Molkentin et al., 1998). CSX/NKX2-5 is expressed in the adult heart (Komuro and Izumo, 1993), and it has been proposed that CSX/NKX2-5 is involved in generation of cardiac hypertrophy (Akazawa and Komuro, 2003) on the basis of in vivo findings that expression levels of CSX/NKX2-5 were increased in response to hypertrophic stimuli including pressure overload (Thompson et al., 1998) and phenylephrine or isoproterenol (Saadane et al., 1999). Therefore, Cal may be another Ca^{2+}-sensitive effector that translocates into the nucleus like NF-AT transcription factors and it is possible to speculate that Cal may play a certain role in generation of cardiac hypertrophy by modulating transcriptional activity of CSX/NKX2-5.

Cal may function as a signal mediator that links cytoplasmic signals and gene expression

Cal was localized in the cytoplasm at steady state and translocated into the nucleus in response to calcium, and Cal functioned as a transcriptional activator in the nucleus by cooper-

ating with the cardiac transcription factor CSX/NKX2-5. These results indicate a novel function of LIM proteins that link cytoplasmic signals and nuclear gene expression.

Recently, some proteins associated with cell junctions have been reported to be involved in transcriptional regulation. A membrane-associated guanylate kinase, CASK/LIN-2, interacts with a T-box transcription factor, Tbr-1, and stimulates the transcriptional activity of Tbr-1 in the nucleus of mammalian cells (Hsueh et al., 2000). Jun activation domain-binding protein 1, colocalizing with integrin LFA-1, translocates into the nucleus in response to LFA-1 stimulation and acts as a coactivator for AP-1 complex (Bianchi et al., 2000). β-Catenin, linking cadherins to actin cytoskeleton at adherens junctions, interacts with T cell factor to form a transcriptional activator complex in response to Wnt signaling (Barth et al., 1997). Although CRP3/MLP binds to Zyxin and α actinin in the cytoplasm (Louis et al., 1997), forced expression of CRP3/MLP in the nucleus by fusing it to nuclear localization signal led to a cooperative enhancement of the transcriptional activity of MyoD (Kong et al., 1997). Trip6 also acts as a coactivator for v-Rel transcription factor (Zhao et al., 1999). However, it remains unclear how subcellular localization of CRP3/MLP and trip6 is regulated. We first clarify the molecular mechanism of how the cytoplasmic LIM protein is translocated into the nucleus and functions as a transcriptional activator.

Cal promotes cardiac differentiation in P19CL6 cells

Mouse P19CL6 cells, derived from P19 embryonal carcinoma cells, are used as a good in vitro system for molecular analysis of cardiac differentiation. In the presence of 1% DMSO, mouse P19CL6 cell efficiently differentiate into spontaneously beating cardiac myocytes that exhibit the biological features recapturing embryonic cardiogenesis in vivo (Monzen et al., 1999, 2001). P19CL6 cells that overexpress nuclear form of Cal (P19CL6-Cal-ΔNES) differentiated into cardiac myocytes more efficiently than the parental P19CL6 cells. In P19CL6-Cal-ΔNES cells, expression levels of *SERCA2*, *calreticulin*, *connexin43*, *ANP*, and *cardiac troponin T* were up-regulated, which convey properties characteristic of cardiomyocytes. Expression levels of cardiac transcription factor *MEF2C* did not change, whereas expression levels of *GATA-4* were increased. Although there has been no evidence indicating that *GATA-4* is a downstream target for CSX/NKX2-5, it is possible that expression of *GATA-4* is up-regulated through undefined functions of Cal. Up-regulation of *GATA-4* might have an influence on myocardial cell differentiation in P19CL6-Cal-ΔNES. These results leave an open question whether the nuclear target for Cal is solely CSX/NKX2-5. However, based on the up-regulated expression of the target genes for CSX/NKX2-5, it is reasonable to assume that cooperation of CSX/NKX2-5 and Cal promoted cardiac differentiation in P19CL6 cells. Our present studies elucidate a novel role of LIM proteins in cardiac development as a transcriptional activator, and suggest that fine-tuned gene expression during cardiogenesis is orchestrated by multiprotein complex including LIM proteins as well as transcription factors.

Materials and methods

Molecular cloning of Cal

We performed a yeast two-hybrid screening using the MATCHMAKER Two-Hybrid System (CLONTECH Laboratories, Inc.) as described previously (Hiroi et al., 2001). The plasmid pGBT9-CSX, which encodes the GAL4 DNA-binding domain fused to the human CSX/NKX2-5, was used as a bait in screening of a human heart MATCHMAKER cDNA Library (CLONTECH Laboratories, Inc.). One clone containing a fragment of CAL cDNA was scored positive, and the full-length mouse Cal cDNA was obtained by screening a mouse heart cDNA library (Stratagene).

Northern blot, RT-PCR, and in situ hybridization analysis

For Northern blot analysis, total RNA was hybridized with cDNA corresponding to 3'-UTR of *Cal*. Probes for *GATA-4*, *MEF2C*, *connexin 43*, and *SERCA2* were described previously (Hiroi et al., 2001). A probe for *calreticulin* was a gift from M. Michalak (University of Alberta, Alberta, Canada). RT-PCR analysis for *ANP* expression was performed as described previously (Hiroi et al., 2001). Digoxygenin labeled riboprobes were synthesized by using the 1.5-kb *Cal* cDNA, and RNA in situ hybridization was performed as described previously (Akazawa et al., 2000).

Plasmids construction

The following plasmids were described previously: the expression vectors of CSX/NKX2-5 (pEFSA-HA-CSX), GATA-4 (pSSRa-hGATA4), and Tbx-5 (pcDNA3-Tbx5); the luciferase reporters containing the *ANP* promoter (ANP[600]-Luc and ANP[2600]-Luc); and multimerized CSX-binding sites (4×TTF-Luc; Shiojima et al., 1999; Hiroi et al., 2001). FLAG-tagged Cal was subcloned into pCAGGS vector (pCAGGS-FLAG-Cal; Niwa et al., 1991; Aoki et al., 2000). pCAGGS vector was provided by J. Miyazaki (Osaka University Graduate School of Medicine, Suita, Japan) and T. Kobayashi and O. Hino (The Cancer Institute, Japanese Foundation for Cancer Research, Tokyo, Japan). Cal derivatives were subcloned into pcDNA3.1 (Invitrogen) and pBIND (Promega) for in vitro transcription and translation and expression of GAL4-fusion protein, respectively. For deletion analyses, the following Cal derivatives were subcloned into the corresponding vectors: Cal-ΔLIM1 (1-184, 221-375), Cal-ΔLIM2 (1-244, 279-375), Cal-ΔLIM3 (1-307, 345-375), Cal-ΔLIM123 (1-184), Cal-LIM123 (185-375), Cal-LIM23 (245-375), and Cal-ΔNES (1-121, 135-375).

Cell culture, transfection, and reporter gene assay

Primary cultures of cardiac myocytes were prepared from ventricles of 1-d-old Wistar rats as described previously (Kudoh et al., 1997). Transient transfections were performed by standard calcium phosphate methods. For reporter gene assays, pRL-SV40 (Promega) was cotransfected as an internal control. Luciferase activities were measured as described previously (Shiojima et al., 1999). P19CL6 cells were cultured as described previously (Monzen et al., 1999). To isolate the permanent cell lines, P19CL6 cells were transfected with pcDNA3.1-Cal and pcDNA3.1-Cal-ΔNES by the lipofection method (TfxTM reagents; Promega). Stable transformants were selected with 400 μg/ml of neomycin (G418; Sigma-Aldrich).

Coimmunoprecipitation experiment

We performed a coimmunoprecipitation experiment as described previously (Shiojima et al., 1999). COS-7 cells were transiently transfected with expression plasmids of pEFSA-HA-CSX and pCAGGS-FLAG-Cal or pCAGGS-FLAG-CalΔNES. For preparation of the cytoplasmic fraction, transfected cells were lysed in digitonin buffer (20 mM Hepes/KOH, pH 7.5, 150 mM NaCl, 1 mM EDTA, and 50 μg/ml digitonin) on ice for 10 min. The lysates were centrifuged at 1,000 *g* and the supernatant was collected as the cytoplasmic fraction. The pellets were resuspended Triton buffer (20 mM Hepes/KOH, pH 7.5, 150 mM NaCl, 1 mM EDTA, and 10 mg/ml Triton X-100) and the lysates were used as the nuclear fraction. Protein samples were subjected to immunoprecipitation with the anti-FLAG mAb M2 (KODAK), fractionated by 10% SDS-PAGE, and immunoblotted with the rabbit polyclonal anti-HA antibody (Santa Cruz Biotechnology, Inc.). HRP-conjugated anti-rabbit IgG antibody was used as the secondary antibody and immune complex was detected by the ECL detection kit (Amersham Biosciences).

GST pull-down assay

We performed GST pull-down assays as described previously (Shiojima et al., 1999). GST fusion protein of CSX/NKX2-5 has been described previously. cDNA fragment corresponding to the full length of Cal was subcloned in frame into the EcoRI site of pGEX-3X (Amersham Biosciences). CSX/NKX2-5 derivatives (Shiojima et al., 1999) and Cal derivatives, subcloned

into pcDNA3.1 vector (Invitrogen), were labeled with [^{35}S]methionine by the TNT Quick Coupled Transcription/Translation Systems (Promega). GST and GST fusion proteins immobilized on glutathione-Sepharose 4B beads were mixed with in vitro–translated proteins. Bound proteins were fractionated by SDS-PAGE and visualized by autoradiography.

Immunostaining

Rat neonatal cardiac myocytes or HeLa cells were transfected with the expression vector of Cal and Cal mutants. Cells were stained with the anti-FLAG mAb M2 (KODAK), and visualized with FITC-labeled anti–mouse IgG (CAPPEL). Calcium ionophore A23187 was purchased from Sigma-Aldrich. Differentiated P19CL6 cells were stained with anticardiac troponin T mAb (Deutsche Sammlung von Mikroorganismen und Zellkulturen GmbH) and visualized with Cy3-labeled anti–mouse IgG (CHEMICON International, Inc.). The cells were double stained using rhodamine-phalloidin (Molecular Probes) or TO-PRO-3 (Molecular Probes).

Nuclear export assays

Nuclear export assays were performed as described previously (Henderson, 2000). pRev(1.4)-NES-EGFP plasmid was constructed by subcloning the NES of Cal between BamHI and AgeI sites of pRev(1.4)-EGFP plasmid (provided by B.R. Henderson, Westmead Institute for Cancer Research, Sydney, Australia). The NES of Cal was amplified by PCR using specific primers (5′-AGGGAAGCCCCCACCCCCGCCTC-3′, and 5′-GGTGGGGGCTTCCCTG-GTAAGACA-3′). Actinomycin D (Sigma-Aldrich) was added at 5 mg/ml to prevent nucleolar association of Rev protein. LMB was provided by M. Yoshida (The University of Tokyo, Tokyo, Japan).

Acquisition and processing of images

For light microscopic analysis (Fig. 1 C), images were acquired by a stereomicroscope (MZ12; objective lens, Plan 1.0×; Leica) and captured by DC100 program (Leica), or by a light microscope (Axioskop 2 plus; objective lens, Plan-Neofluar 2.5×/0.075; Carl Zeiss MicroImaging, Inc.) and captured by Axio Cam CCD camera and Axio Vision 3.0 imaging system (Carl Zeiss MicroImaging, Inc.). For immunofluorescence microscopic analysis, images were acquired by a laser-scanning microscope (model Eclipse E600; Nikon) using Plan-Fluor 10×/0.30 (Fig. 7 B), Plan-Fluor 40×/0.75 (Fig. 6 A), and Plan-Apo 60×A/1.40 oil (Fig. 5). Radiance 2000 confocal scanning system (Bio-Rad Laboratories) was used.

Accession no.

The deduced amino acid sequence of mouse Cal was deposited in GenBank/EMBL/DDBJ accession no. AF513359.

We thank Ms. R. Kobayashi, E. Fujita, and M. Watanabe for their excellent technical assistance.

This work was supported in part by grants from the Japanese Ministry of Education, Science, Sports, and Culture, and Japan Health Sciences Foundation (JHSF; to I. Komuro), Japanese Heart Foundation and Kanae Foundation for Life and Sociomedical Science (to H. Akazawa). H. Akazawa is a Research Resident for Research on Human Genome, Tissue Engineering Food Biotechnology of JHSF.

Submitted: 26 September 2003
Accepted: 29 December 2003

References

Akazawa, H., and I. Komuro. 2003. Roles of cardiac transcription factors in cardiac hypertrophy. *Circ. Res.* 92:1079–1088.

Akazawa, H., I. Komuro, Y. Sugitani, Y. Yazaki, R. Nagai, and T. Noda. 2000. Targeted disruption of the homeobox transcription factor Bapx1 results in lethal skeletal dysplasia with asplenia and gastroduodenal malformation. *Genes Cells.* 5:499–513.

Aoki, H., J. Hayashi, M. Moriyama, Y. Arakawa, and O. Hino. 2000. Hepatitis C virus core protein interacts with 14-3-3 protein and activates the kinase Raf-1. *J. Virol.* 74:1736–1741.

Arber, S., and P. Caroni. 1996. Specificity of single LIM motifs in targeting and LIM/LIM interactions in situ. *Genes Dev.* 10:289–300.

Arber, S., G. Halder, and P. Caroni. 1994. Muscle LIM protein, a novel essential regulator of myogenesis, promotes myogenic differentiation. *Cell.* 79: 221–231.

Arber, S., J.J. Hunter, J. Ross, Jr., M. Hongo, G. Sansig, J. Borg, J.C. Perriard, K.R. Chien, and P. Caroni. 1997. MLP-deficient mice exhibit a disruption of cardiac cytoarchitectural organization, dilated cardiomyopathy, and heart failure. *Cell.* 88:393–403.

Bach, I. 2000. The LIM domain: regulation by association. *Mech. Dev.* 91:5–17.

Barth, A.I., I.S. Nathke, and W.J. Nelson. 1997. Cadherins, catenins and APC protein: interplay between cytoskeletal complexes and signaling pathways. *Curr. Opin. Cell Biol.* 9:683–690.

Beckerle, M.C. 1997. Zyxin: zinc fingers at sites of cell adhesion. *Bioessays.* 19: 949–957.

Bianchi, E., S. Denti, A. Granata, G. Bossi, J. Geginat, A. Villa, L. Rogge, and R. Pardi. 2000. Integrin LFA-1 interacts with the transcriptional co-activator JAB1 to modulate AP-1 activity. *Nature.* 404:617–621.

Bruneau, B.G., G. Nemer, J.P. Schmitt, F. Charron, L. Robitaille, S. Caron, D.A. Conner, M. Gessler, M. Nemer, C.E. Seidman, and J.G. Seidman. 2001. A murine model of Holt-Oram syndrome defines roles of the T-box transcription factor Tbx5 in cardiogenesis and disease. *Cell.* 106:709–721.

Chen, C.Y., and R.J. Schwartz. 1996. Recruitment of the tinman homolog Nkx-2.5 by serum response factor activates cardiac alpha-actin gene transcription. *Mol. Cell. Biol.* 16:6372–6384.

Clapham, D.E. 1995. Calcium signaling. *Cell.* 80:259–268.

Dawid, I.B., J.J. Breen, and R. Toyama. 1998. LIM domains: multiple roles as adapters and functional modifiers in protein interactions. *Trends Genet.* 14: 156–162.

Durocher, D., F. Charron, R. Warren, R.J. Schwartz, and M. Nemer. 1997. The cardiac transcription factors Nkx2-5 and GATA-4 are mutual cofactors. *EMBO J.* 16:5687–5696.

Fornerod, M., M. Ohno, M. Yoshida, and I.W. Mattaj. 1997. CRM1 is an export receptor for leucine-rich nuclear export signals. *Cell.* 90:1051–1060.

Frey, N., T.A. McKinsey, and E.N. Olson. 2000. Decoding calcium signals involved in cardiac growth and function. *Nat. Med.* 6:1221–1227.

Gertler, F.B., K. Niebuhr, M. Reinhard, J. Wehland, and P. Soriano. 1996. Mena, a relative of VASP and *Drosophila* Enabled, is implicated in the control of microfilament dynamics. *Cell.* 87:227–239.

Goyal, R.K., P. Lin, J. Kanungo, A.S. Payne, A.J. Muslin, and G.D. Longmore. 1999. Ajuba, a novel LIM protein, interacts with Grb2, augments mitogen-activated protein kinase activity in fibroblasts, and promotes meiotic maturation of *Xenopus* oocytes in a Grb2- and Ras-dependent manner. *Mol. Cell. Biol.* 19:4379–4389.

Henderson, B.R. 2000. Nuclear-cytoplasmic shuttling of APC regulates beta-catenin subcellular localization and turnover. *Nat. Cell Biol.* 2:653–660.

Hiroi, Y., S. Kudoh, K. Monzen, Y. Ikeda, Y. Yazaki, R. Nagai, and I. Komuro. 2001. Tbx5 associates with Nkx2-5 and synergistically promotes cardiomyocyte differentiation. *Nat. Genet.* 28:276–280.

Hirota, T., T. Morisaki, Y. Nishiyama, T. Marumoto, K. Tada, T. Hara, N. Masuko, M. Inagaki, K. Hatakeyama, and H. Saya. 2000. Zyxin, a regulator of actin filament assembly, targets the mitotic apparatus by interacting with h-warts/LATS1 tumor suppressor. *J. Cell Biol.* 149:1073–1086.

Hobert, O., J.W. Schilling, M.C. Beckerle, A. Ullrich, and B. Jallal. 1996. SH3 domain-dependent interaction of the proto-oncogene product Vav with the focal contact protein zyxin. *Oncogene.* 12:1577–1581.

Hsueh, Y.P., T.F. Wang, F.C. Yang, and M. Sheng. 2000. Nuclear translocation and transcription regulation by the membrane-associated guanylate kinase CASK/LIN-2. *Nature.* 404:298–302.

Kanungo, J., S.J. Pratt, H. Marie, and G.D. Longmore. 2000. Ajuba, a cytosolic LIM protein, shuttles into the nucleus and affects embryonal cell proliferation and fate decisions. *Mol. Biol. Cell.* 11:3299–3313.

Komuro, I., and S. Izumo. 1993. Csx: a murine homeobox-containing gene specifically expressed in the developing heart. *Proc. Natl. Acad. Sci. USA.* 90: 8145–8149.

Kong, Y., M.J. Flick, A.J. Kudla, and S.F. Konieczny. 1997. Muscle LIM protein promotes myogenesis by enhancing the activity of MyoD. *Mol. Cell. Biol.* 17:4750–4760.

Kudo, N., B. Wolff, T. Sekimoto, E.P. Schreiner, Y. Yoneda, M. Yanagida, S. Horinouchi, and M. Yoshida. 1998. Leptomycin B inhibition of signal-mediated nuclear export by direct binding to CRM1. *Exp. Cell Res.* 242:540–547.

Kudoh, S., I. Komuro, T. Mizuno, T. Yamazaki, Y. Zou, I. Shiojima, N. Takekoshi, and Y. Yazaki. 1997. Angiotensin II stimulates c-Jun NH2-terminal kinase in cultured cardiac myocytes of neonatal rats. *Circ. Res.* 80:139–146.

Kuersten, S., M. Ohno, and I.W. Mattaj. 2001. Nucleocytoplasmic transport: Ran, beta and beyond. *Trends Cell Biol.* 11:497–503.

Lee, Y., T. Shioi, H. Kasahara, S.M. Jobe, R.J. Wiese, B.E. Markham, and S. Izumo. 1998. The cardiac tissue-restricted homeobox protein Csx/Nkx2.5 physically associates with the zinc finger protein GATA4 and cooperatively activates atrial natriuretic factor gene expression. *Mol. Cell. Biol.* 18:3120–3129.

Lints, T.J., L.M. Parsons, L. Hartley, I. Lyons, and R.P. Harvey. 1993. Nkx-2.5: a novel murine homeobox gene expressed in early heart progenitor cells and their myogenic descendants. *Development.* 119:969.

Louis, H.A., J.D. Pino, K.L. Schmeichel, P. Pomies, and M.C. Beckerle. 1997. Comparison of three members of the cysteine-rich protein family reveals functional conservation and divergent patterns of gene expression. *J. Biol. Chem.* 272:27484–27491.

Lyons, I., L.M. Parsons, L. Hartley, R. Li, J.E. Andrews, L. Robb, and R.P. Harvey. 1995. Myogenic and morphogenetic defects in the heart tubes of murine embryos lacking the homeo box gene Nkx2-5. *Genes Dev.* 9:1654–1666.

Mahoney, N.M., P.A. Janmey, and S.C. Almo. 1997. Structure of the profilin-poly-L-proline complex involved in morphogenesis and cytoskeletal regulation. *Nat. Struct. Biol.* 4:953–960.

Mattaj, I.W., and L. Englmeier. 1998. Nucleocytoplasmic transport: the soluble phase. *Annu. Rev. Biochem.* 67:265–306.

Missero, C., M.T. Pirro, S. Simeone, M. Pischetola, and R. Di Lauro. 2001. The DNA glycosylase T:G mismatch-specific thymine DNA glycosylase represses thyroid transcription factor-1-activated transcription. *J. Biol. Chem.* 276: 33569–33575.

Molkentin, J.D., J.R. Lu, C.L. Antos, B. Markham, J. Richardson, J. Robbins, S.R. Grant, and E.N. Olson. 1998. A calcineurin-dependent transcriptional pathway for cardiac hypertrophy. *Cell.* 93:215–228.

Monzen, K., I. Shiojima, Y. Hiroi, S. Kudoh, T. Oka, E. Takimoto, D. Hayashi, T. Hosoda, A. Habara-Ohkubo, T. Nakaoka, et al. 1999. Bone morphogenetic proteins induce cardiomyocyte differentiation through the mitogen-activated protein kinase kinase kinase TAK1 and cardiac transcription factors Csx/Nkx-2.5 and GATA-4. *Mol. Cell. Biol.* 19:7096–7105.

Monzen, K., Y. Hiroi, S. Kudoh, H. Akazawa, T. Oka, E. Takimoto, D. Hayashi, T. Hosoda, M. Kawabata, K. Miyazono, et al. 2001. Smads, TAK1, and their common target ATF-2 play a critical role in cardiomyocyte differentiation. *J. Cell Biol.* 153:687–698.

Niwa, H., K. Yamamura, and J. Miyazaki. 1991. Efficient selection for high-expression transfectants with a novel eukaryotic vector. *Gene.* 108:193–199.

Nix, D.A., and M.C. Beckerle. 1997. Nuclear-cytoplasmic shuttling of the focal contact protein, zyxin: a potential mechanism for communication between sites of cell adhesion and the nucleus. *J. Cell Biol.* 138:1139–1147.

Ohno, M., M. Fornerod, and I.W. Mattaj. 1998. Nucleocytoplasmic transport: the last 200 nanometers. *Cell.* 92:327–336.

Petit, M.M., R. Mols, E.F. Schoenmakers, N. Mandahl, and W.J. Van de Ven. 1996. LPP, the preferred fusion partner gene of HMGIC in lipomas, is a novel member of the LIM protein gene family. *Genomics.* 36:118–129.

Petit, M.M., J. Fradelizi, R.M. Golsteyn, T.A. Ayoubi, B. Menichi, D. Louvard, W.J. Van de Ven, and E. Friederich. 2000. LPP, an actin cytoskeleton protein related to zyxin, harbors a nuclear export signal and transcriptional activation capacity. *Mol. Biol. Cell.* 11:117–129.

Prehoda, K.E., D.J. Lee, and W.A. Lim. 1999. Structure of the enabled/VASP homology 1 domain-peptide complex: a key component in the spatial control of actin assembly. *Cell.* 97:471–480.

Renfranz, P.J., and M.C. Beckerle. 2002. Doing (F/L)PPPPs: EVH1 domains and their proline-rich partners in cell polarity and migration. *Curr. Opin. Cell Biol.* 14:88–103.

Saadane, N., L. Alpert, and L.E. Chalifour. 1999. Expression of immediate early genes, GATA-4, and Nkx-2.5 in adrenergic-induced cardiac hypertrophy and during regression in adult mice. *Br. J. Pharmacol.* 127:1165–1176.

Sadler, I., A.W. Crawford, J.W. Michelsen, and M.C. Beckerle. 1992. Zyxin and cCRP: two interactive LIM domain proteins associated with the cytoskeleton. *J. Cell Biol.* 119:1573–1587.

Schlessinger, J. 2000. Cell signaling by receptor tyrosine kinases. *Cell.* 103:211–225.

Schott, J.J., D.W. Benson, C.T. Basson, W. Pease, G.M. Silberbach, J.P. Moak, B.J. Maron, C.E. Seidman, and J.G. Seidman. 1998. Congenital heart disease caused by mutations in the transcription factor NKX2-5. *Science.* 281: 108–111.

Shiojima, I., I. Komuro, T. Oka, Y. Hiroi, T. Mizuno, E. Takimoto, K. Monzen, R. Aikawa, H. Akazawa, T. Yamazaki, et al. 1999. Context-dependent transcriptional cooperation mediated by cardiac transcription factors Csx/Nkx-2.5 and GATA-4. *J. Biol. Chem.* 274:8231–8239.

Thompson, J.T., M.S. Rackley, and T.X. O'Brien. 1998. Upregulation of the cardiac homeobox gene Nkx2-5 (CSX) in feline right ventricular pressure overload. *Am. J. Physiol.* 274:H1569–H1573.

Wang, Y., and T.D. Gilmore. 2001. LIM domain protein Trip6 has a conserved nuclear export signal, nuclear targeting sequences, and multiple transactivation domains. *Biochim. Biophys. Acta.* 1538:260–272.

Yi, J., and M.C. Beckerle. 1998. The human TRIP6 gene encodes a LIM domain protein and maps to chromosome 7q22, a region associated with tumorigenesis. *Genomics.* 49:314–316.

Zhao, M.K., Y. Wang, K. Murphy, J. Yi, M.C. Beckerle, and T.D. Gilmore. 1999. LIM domain-containing protein trip6 can act as a coactivator for the v-Rel transcription factor. *Gene Expr.* 8:207–217.

Available online at www.sciencedirect.com
SCIENCE DIRECT®
Neurochemistry International 44 (2004) 497–503
NEUROCHEMISTRY International
www.elsevier.com/locate/neuint

Simultaneous monitoring of acetylcholine and catecholamine release in the in vivo rat adrenal medulla

Tsuyoshi Akiyama [a,*], Toji Yamazaki [a], Hidezo Mori [a], Kenji Sunagawa [b]

[a] *Department of Cardiac Physiology, National Cardiovascular Center Research Institute, 5-7-1 Fujishiro-dai, Suita, Osaka 565-8565, Japan*
[b] *Department of Cardiovascular Dynamics, National Cardiovascular Center Research Institute, Suita, Osaka 565-8565, Japan*

Received 20 May 2003; accepted 3 September 2003

Abstract

To simultaneously monitor acetylcholine release from pre-ganglionic adrenal sympathetic nerve endings and catecholamine release from post-ganglionic adrenal chromaffin cells in the in vivo state, we applied microdialysis technique to anesthetized rats. Dialysis probe was implanted in the left adrenal medulla and perfused with Ringer's solution containing neostigmine (a cholinesterase inhibitor). After transection of splanchnic nerves, we electrically stimulated splanchnic nerves or locally administered acetylcholine through dialysis probes for 2 min and investigated dialysate acetylcholine, choline, norepinephrine and epinephrine responses. Acetylcholine was not detected in dialysate before nerve stimulation, but substantial acetylcholine was detected by nerve stimulation. In contrast, choline was detected in dialysate before stimulation, and dialysate choline concentration did not change with repetitive nerve stimulation. The estimated interstitial acetylcholine levels and dialysate catecholamine responses were almost identical between exogenous acetylcholine (10 μM) and nerve stimulation (2 Hz). Dialysate acetylcholine, norepinephrine and epinephrine responses were correlated with the frequencies of electrical nerve stimulation, and dialysate norepinephrine and epinephrine responses were quantitatively correlated with dialysate acetylcholine responses. Neither hexamethonium (a nicotinic receptor antagonist) nor atropine (a muscarinic receptor antagonist) affected the dialysate acetylcholine response to nerve stimulation. Microdialysis technique made it possible to simultaneously assess activities of pre-ganglionic adrenal sympathetic nerves and post-ganglionic adrenal chromaffin cells in the in vivo state and provided quantitative information about input–output relationship in the adrenal medulla.

Keywords: Anesthetized rats; Microdialysis; Choline; Norepinephrine; Epinephrine

1. Introduction

Although acetylcholine is one of major neurotransmitters in the peripheral autonomic nervous system as well as central nervous system (Collier, 1977; Fibiger, 1991; Calabresi et al., 2000), it has been difficult to measure endogenous acetylcholine in the in vivo state since acetylcholine released from nerve endings is rapidly degraded by tissue acetylcholinesterase (Taylor and Brown, 1998). Recently, microdialysis technique with improved measurement has made it possible to monitor low levels of acetylcholine in the in vivo central nervous system. In the peripheral autonomic nervous system, we have measured acetylcholine release from post-ganglionic parasympathetic nerve endings using microdialysis technique (Akiyama et al., 1994; Akiyama and Yamazaki, 2000, 2001; Kawada et al., 2001). Little information is, however, available on acetylcholine release from pre-ganglionic autonomic nerve endings in the in vivo state. The assessment of pre-ganglionic autonomic nerve activities is important for understanding the autonomic ganglionic transmission under physiological and pathophysiological conditions.

Adrenal medulla is one candidate suitable for investigating acetylcholine release from pre-ganglionic autonomic nerve endings (Holman et al., 1994). Compared to autonomic ganglia, adrenal gland is solid and suited to microdialysis probe implantation. Furthermore, microdialysis technique in the adrenal medulla provides a distinct advantage to monitor catecholamine release from adrenal medulla following acetylcholine release. Thus, we consider it possible to simultaneously assess pre- and post-ganglionic sympathetic nerve activities by monitoring acetylcholine and catecholamine release in the adrenal medulla.

In the present study, we applied the microdialysis technique to the adrenal medulla of anesthetized rats and tested the suitability of microdialysis technique to simultaneously

* Corresponding author. Tel.: +81-6-6833-5012x2380; fax: +81-6-6872-8092.
E-mail address: takiyama@ri.ncvc.go.jp (T. Akiyama).

0197-0186/$ – see front matter © 2003 Elsevier Ltd. All rights reserved.
doi:10.1016/j.neuint.2003.09.001

monitor acetylcholine and catecholamine release from adrenal medulla.

2. Materials and methods

2.1. Animal preparation

The investigation conforms with the *Guide for the Care and Use of Laboratory Animals* published by the US National Institutes of Health (NIH Publication No. 85-23, revised 1996). Adult male Wistar rats weighing 390–460 g were anesthetized with pentobarbital sodium (50–55 mg/kg i.p.). The rats were ventilated with a constant-volume respirator using room air mixed with oxygen. The left femoral artery and vein were cannulated for monitoring arterial blood pressure and administration of anesthetic, respectively. The level of anesthesia was maintained with a continuous intravenous infusion of pentobarbital sodium (15–25 mg/(kg h) i.v.). Electrocardiogram was monitored for recording heart rate. A thermostatic heating pad was used to keep the esophageal temperature within a range of 37–38 °C. With the animal in the lateral position, the left adrenal gland and left splanchnic nerve were exposed by a subcostal flank incision, and the left splanchnic nerve was transected. In protocols requiring nerve stimulation, shielded bipolar stainless steel electrodes were applied to the distal end of the nerve, which was then stimulated with a digital stimulator (SEN-7203, Nihon Kohden, Japan) with a rectangular pulse (10 V and 1 ms in duration).

2.2. Dialysis technique

The materials of the dialysis probe were the same as those used in our previous dialysis experiments (Akiyama et al., 2003). Briefly, each end of the dialysis fiber (0.31 mm o.d., and 0.20 mm i.d.; PAN-1200 50,000 mol. wt. cutoff, Asahi Chemical, Japan) was inserted into the polyethylene tube (25 cm length, 0.50 mm o.d., and 0.20 mm i.d.; SP-8) and glued. The length of the dialysis fiber exposed was 3 mm. At perfusion speed of 10 μl/min, in vitro recovery rates of acetylcholine, choline, norepinephrine, and epinephrine were (%): 3.08 ± 0.04, 2.93 ± 0.10, 2.09 ± 0.03, and 2.16 ± 0.03, respectively (number of dialysis probes: 3).

The dialysis probe was implanted in the medulla of the left adrenal gland and perfused with Ringer's solution containing the cholinesterase inhibitor, neostigmine (10 μM) at a speed of 10 μl/min using a microinjection pump (CMA/100, Carnegie Medicin, Sweden). Ringer's solution consisted of (in mM) 147.0 NaCl, 4.0 KCl, 2.25 $CaCl_2$. All pharmacological agents tested were locally administered by perfusion through the dialysis probe after being dissolved in Ringer's solution. One sampling period was 2 min (one sample volume = 20 μl). We started the protocols followed by a stabilization period of 3–4 h. Catecholamine release was evoked by 2 min-local administration of acetylcholine or 2 min-electrical stimulation of left splanchnic nerves. In protocols requiring repeated nerve stimulation, electrical stimulation was performed at 30 min-intervals. Taking the dead space volume into account, we continuously collected three dialysate samples per pharmacological or electrical stimulation: one before, one during, and one after stimulation. We subtracted the dialysate acetylcholine, norepinephrine, or epinephrine contents in control from those during stimulation, and expressed these values as indices of dialysate acetylcholine, norepinephrine or epinephrine response to stimulation.

Half of the dialysate sample was injected into high-performance liquid chromatography for the measurement of acetylcholine and choline (Akiyama et al., 1994), and the remaining half was injected into another high-performance liquid chromatography for the measurement of norepinephrine and epinephrine (Akiyama et al., 1991).

2.3. Experimental protocols

2.3.1. Protocol 1

We repeated stimulations of splanchnic nerves at 2 and 4 Hz twice and examined dialysate acetylcholine, choline and catecholamine responses to nerve stimulation and their reproducibility in five rats.

2.3.2. Protocol 2

To compare the estimated interstitial acetylcholine levels between administration of acetylcholine and nerve stimulation, we locally administered acetylcholine (10 μM) in five rats and stimulated splanchnic nerves at 2 Hz in five other rats. The concentration of exogenous acetylcholine was determined to obtain a similar dialysate catecholamine response to nerve stimulation at 2 Hz.

2.3.3. Protocol 3

We raised stepwise the frequency of nerve stimulation from 2 to 4, 10, 20 Hz and examined dialysate acetylcholine and catecholamine responses in five rats. In addition, to examine the input–output relationship in the adrenal medulla, we analyzed the relationship between dialysate acetylcholine and catecholamine responses of five rats.

2.3.4. Protocol 4

We examined the effects of cholinergic receptor antagonists on dialysate acetylcholine and catecholamine responses. Nerve stimulations at 2 and 4 Hz were performed before and after 30 min-local administration of cholinergic receptor antagonists. We tested the nicotinic receptor antagonist, hexamethonium bromide (1 mM) in five rats or the muscarinic receptor antagonist, atropine sulfate (10 μM) in five other rats.

2.4. Statistical methods

To examine the effect of nerve stimulation and pharmacological agents, we analyzed heart rate and mean

arterial pressure, and dialysate acetylcholine, choline, norepinephrine and epinephrine responses, using one- or two-way analysis of variance with repeated measures. When statistical significance was detected, the Newman–Keuls test was applied (Winer, 1971). Statistical significance was defined as $P < 0.05$. Values are presented as mean ± S.E.

3. Results

The experiments were carried in anesthetized rats and had been performed in the presence of neostigmine. Local administration of pharmacological agents did not influence heart rate or mean arterial pressure in any of the protocols. In protocol 3 ($n = 5$), nerve stimulation at 2 Hz decreased heart rate from 420 ± 8 to 397 ± 8 beats/min ($P < 0.05$) and increased mean arterial pressure from 125 ± 4 to 136 ± 3 mmHg ($P < 0.05$). Heart rate and mean arterial pressure recovered after cessation of stimulation. Nerve stimulation at 4, 10 and 20 Hz decreased heart rate to 396±9, 393±7 and 392 ± 9 beats/min, respectively, and increased mean arterial pressure to 134±3, 141±3, and 142±3 mmHg, respectively. In the other protocols, nerve stimulation at 2 or 4 Hz evoked the same responses of heart rate and mean arterial pressure.

3.1. Dialysate acetylcholine and catecholamine

3.1.1. Protocol 1

As shown in the *upper panel* of Fig. 1 ($n = 5$), acetylcholine was not detected in dialysate before nerve stimulation, but substantial acetylcholine was detected in dialysate by nerve stimulation. In contrast, choline, norepinephrine, and epinephrine were detected in dialysate before stimulation. Dialysate choline concentration did not change with repetitive nerve stimulation. Dialysate norepinephrine and epinephrine concentrations increased with nerve stimulation. Stimulation at the same frequency elicited almost identical responses on repetition.

3.1.2. Protocol 2

Using in vitro recovery rate of acetylcholine (3.08%), the estimated interstitial acetylcholine levels were 308 nM in acetylcholine infusion (10 μM, $n = 5$) and 276 ± 15 nM in nerve stimulation (2 Hz, $n = 5$; Fig. 1, *lower panel*). There was no statistical difference in the estimated interstitial acetylcholine levels and dialysate catecholamine responses between the two groups.

3.1.3. Protocol 3

When the frequency of nerve stimulation was increased from 2 to 20 Hz, dialysate acetylcholine, norepinephrine and epinephrine responses were enhanced ($n = 5$; Fig. 2, *upper panel*). We plotted the relationship between dialysate catecholamine response (ordinate) and dialysate acetylcholine response (abscissa) of five rats (Fig. 2, *lower panel*). Dialysate norepinephrine and epinephrine responses correlated with dialysate acetylcholine responses.

3.1.4. Protocol 4

At both 2 and 4 Hz of nerve stimulation, hexamethonium suppressed dialysate norepinephrine and epinephrine responses, but did not affect acetylcholine response ($n = 5$; Fig. 3, *upper panel*). Atropine suppressed epinephrine response at both 2 and 4 Hz of nerve stimulation, but did not affect norepinephrine and acetylcholine responses ($n = 5$; Fig. 3, *lower panel*).

4. Discussion

By now, simultaneous monitoring of adrenal acetylcholine and catecholamine release has been limited to only a few studies using perfused adrenal gland. Collier et al. (1984) measured endogenous acetylcholine and catecholamine effluxes from perfused cat adrenal gland. O'Farrell et al. (1997) preloaded bovine adrenal glands with [^{3}H]-choline and measured the subsequent efflux of [^{3}H]-labelled compound as an index of acetylcholine release and catecholamine efflux. In the present in vivo study, dialysate acetylcholine and catecholamine responses served as indices of acetylcholine release from splanchnic nerve endings and catecholamine release from adrenal medulla, respectively. This simultaneous monitoring implies quantitative measurement of pre- and post-ganglionic neurotransmitter release at the adrenal medulla.

4.1. Source of dialysate acetylcholine

The stimulation of splanchnic nerve induced acetylcholine release from pre-ganglionic nerve endings and increased dialysate acetylcholine concentration. It has been demonstrated that adrenal gland receives parasympathetic efferent and afferent innervation (Coupland et al., 1989; Niijima, 1992; Parker et al., 1993). Branches of parasympathetic efferent nerves conduct through celiac nerves, celiac ganglion and splanchnic nerves to adrenal nerves (Niijima, 1992). In the present study, we electrically stimulated the portion just distal to the sympathetic chain and proximal to the celiac ganglion. This portion does not contain branches of parasympathetic efferent nerves. After transection of splanchnic nerves, basal dialysate acetylcholine was less than the detection limit of high performance liquid chromatography (10 fmol), and substantial acetylcholine was detected in dialysate during the stimulation of this portion. Thus, most of the detected acetylcholine in dialysate derives from pre-ganglionic sympathetic nerve endings.

4.2. Interstitial choline levels in the adrenal medulla

Under physiological conditions, there is enough acetylcholinesterase activity in splanchnic nerve endings, chromaffin cells, and interstitial cells (Coupland, 1965; Palkama, 1967; Lewis and Shute, 1969; Somogyi et al., 1975). Released acetylcholine is degraded to choline and acetate by

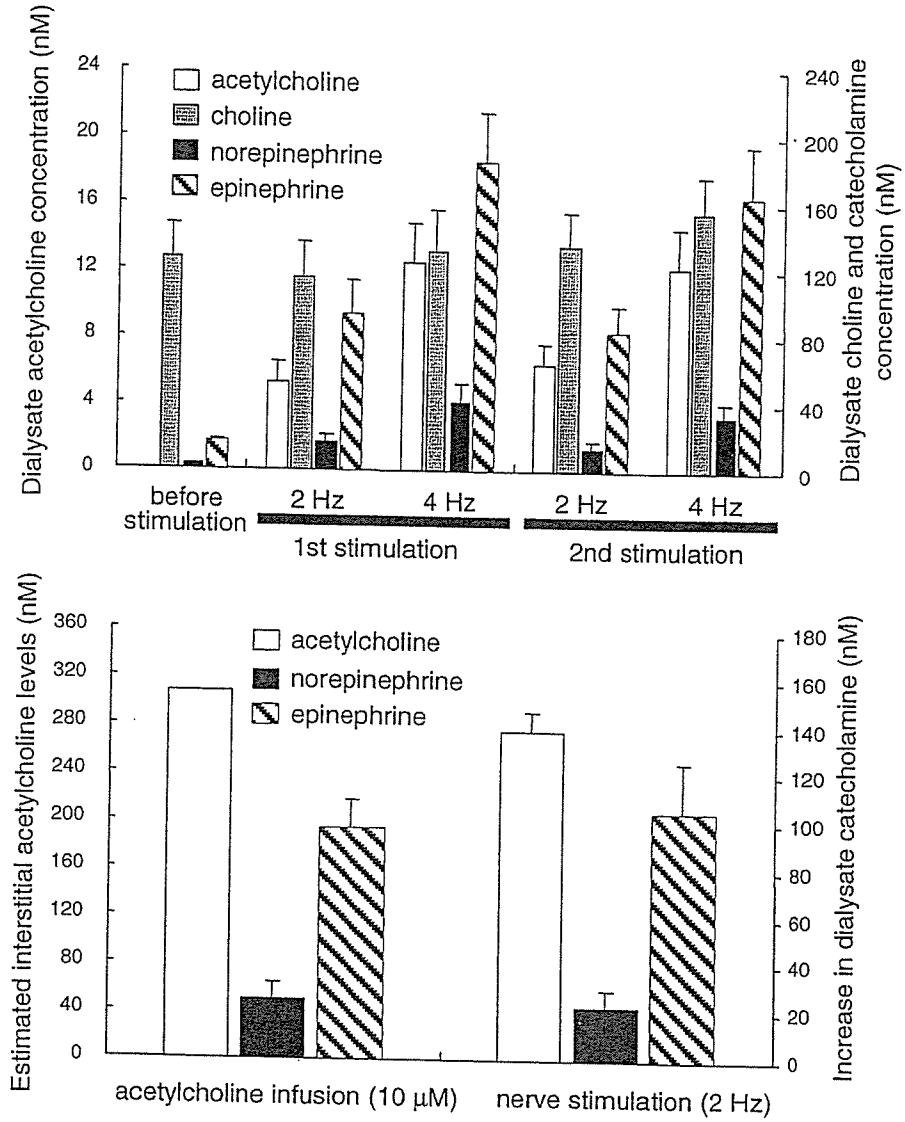

Fig. 1. (*Upper panel*) Acetylcholine was not detected in dialysate before nerve stimulation, but substantial acetylcholine was detected in dialysate by nerve stimulation (5 ± 1 nM at 2 Hz and 12 ± 2 nM at 4 Hz). Dialysate choline concentration did not change with nerve stimulation. Dialysate norepinephrine and epinephrine concentrations increased with nerve stimulation (17 ± 5 and 94 ± 20 nM at 2 Hz, respectively, and 41 ± 12 and 185 ± 29 nM at 4 Hz, respectively). Stimulation at the same frequency elicited almost identical responses on repetition, $n = 5$. Values are mean ± S.E. (*Lower panel*) There was no statistical difference in the estimated interstitial acetylcholine levels and dialysate catecholamine responses between acetylcholine infusion (10 μM, $n = 5$) and nerve stimulation (2 Hz, $n = 5$). Values are mean ± S.E.

acetylcholinesterase. Interstitial choline is carried into the nerve endings through neuronal transporters and used as a precursor for synthesis of acetylcholine (Taylor and Brown, 1998). In in vitro perfused experiments, continuous administration of choline sustains the synthesis and release of acetylcholine from nerve endings. In the present study, the concentration of dialysate choline was more than 10 times that of dialysate acetylcholine during nerve stimulation, and repetitive acetylcholine release did not induce a decrease in dialysate choline concentration. Moreover, nerve stimulation elicited almost identical responses of dialysate acetylcholine on repetition. These results indicate that repetitive acetylcholine release did not decrease interstitial choline levels and did not affect release of acetylcholine. Thus, under in vivo conditions, adrenal interstitial choline levels may be sufficiently high to sustain acetylcholine synthesis in the pre-ganglionic nerve endings.

4.3. Catecholamine release induced by endogenous and exogenous acetylcholine

Either exogenous or endogenous acetylcholine evokes catecholamine release by activating cholinergic receptors on the surface of chromaffin cells (Douglas, 1975). The interstitial acetylcholine levels serves as an index of input into chromaffin cells. We examined whether the estimated interstitial acetylcholine levels were identical between exogenous acetylcholine and nerve stimulation when

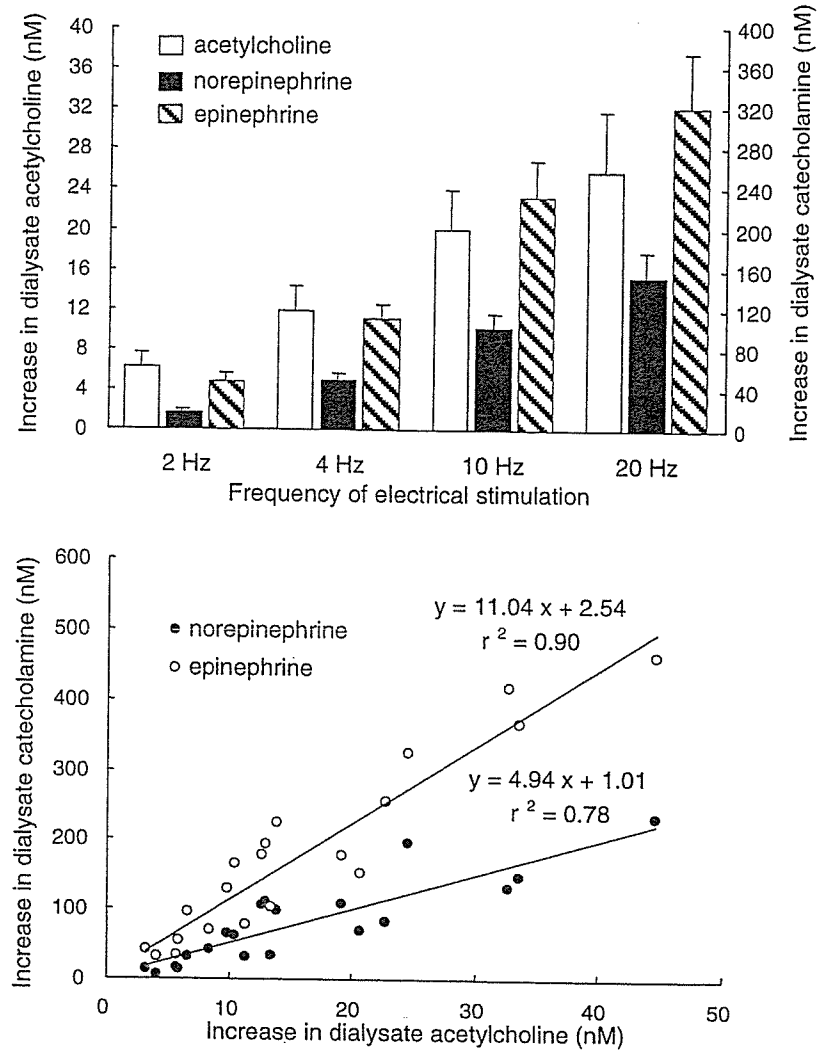

Fig. 2. (*Upper panel*) Dialysate acetylcholine response was enhanced from 6 ± 1 to 26 ± 6 nM when the frequency of nerve stimulation was increased from 2 to 20 Hz. Similarly, dialysate norepinephrine and epinephrine responses were enhanced from 16 ± 4 to 152 ± 26 nM and 48 ± 9 to 321 ± 54 nM, respectively, $n = 5$. Values are mean ± S.E. (*Lower panel*) The relationship between dialysate catecholamine response (*ordinate*) and dialysate acetylcholine response (*abscissa*) of five rats. Dialysate norepinephrine and epinephrine responses correlated with dialysate acetylcholine responses. These relations were expressed by regression equations with correlation coefficients of $y = 4.94x + 1.01$, $r^2 = 0.78$, and $y = 11.04x + 2.54$, $r^2 = 0.90$, respectively.

dialysate catecholamine responses were equal. Actually the estimated interstitial acetylcholine levels during nerve stimulation (2 Hz) were identical with those during acetylcholine infusion (10 μM). These data indicate that inputs into chromaffin cells were almost identical between the two stimulations. It could be inferred from this finding that dialysate acetylcholine concentration reflects acetylcholine levels at the surface of chromaffin cells and serves as an index of cholinergic transmission in the adrenal medulla.

4.4. Relationship of acetylcholine and catecholamine release

Dialysate norepinephrine and epinephrine responses were correlated with the frequency of splanchnic nerve stimulation. This norepinephrine and epinephrine release occurred as a consequence of acetylcholine release by splanchnic nerve stimulation. We found a linear relation between dialysate acetylcholine response and dialysate catecholamine responses. This indicates that the input–output relationship in the adrenal medulla is linear over the range of frequency from 2 to 20 Hz. Dialysate acetylcholine response of 1 nM evoked dialysate norepinephrine response of about 5 nM and dialysate epinephrine response of about 11 nM. This relation between dialysate acetylcholine and catecholamine responses could provide quantitative information about the input–output relationship in the adrenal medulla.

4.5. Effects of cholinergic receptor antagonists

It has been suggested that acetylcholine release from pre-ganglionic nerve endings is modulated by pre-synaptic

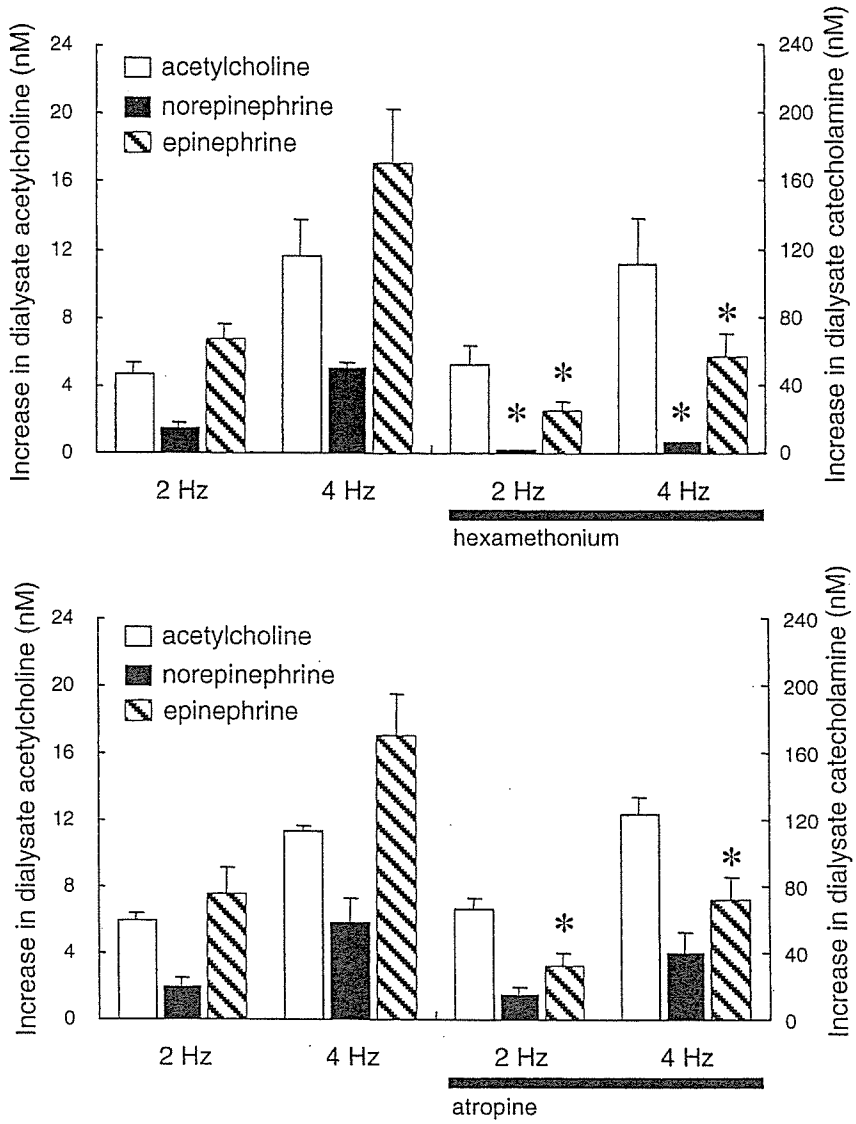

Fig. 3. (*Upper panel*) At both 2 and 4 Hz of nerve stimulation, hexamethonium suppressed dialysate norepinephrine and epinephrine responses, but did not affect acetylcholine response, $n = 5$. Values are mean ± S.E. $^*P < 0.05$ vs. concurrent dialysate norepinephrine or epinephrine response before administration of hexamethonium. (*Lower panel*) At both 2 and 4 Hz of nerve stimulation, atropine suppressed epinephrine response, but did not affect norepinephrine and acetylcholine responses, $n = 5$. Values are mean ± S.E. $^*P < 0.05$ vs. concurrent dialysate norepinephrine or epinephrine response before administration of atropine.

cholinergic autoreceptors (Dujic et al., 1990; Myers and Undem, 1996; Barbara et al., 1998). Neostigmine might induce the activation of pre-synaptic cholinergic receptors by increasing the acetylcholine levels in synaptic regions (Brehm et al., 1992) and suppress acetylcholine release by activating pre-synaptic autoreceptors. In the present study, neither hexamethonium nor atropine affected dialysate acetylcholine response to nerve stimulation at either 2 or 4 Hz. Thus, autoinhibition of acetylcholine release can be considered insignificant in our experimental condition, and dialysate acetylcholine response reflects pre-ganglionic nerve activities. In contrast, hexamethonium suppressed norepinephrine and epinephrine releases by nerve stimulation whereas atropine suppressed only epinephrine release. The muscarinic agonist, muscarine or pilocarpine preferentially enhanced epinephrine release (Douglas and Poisner, 1965; Wakade and Wakade, 1983). These results suggest that both nicotinic and muscarinic receptors exist on the surface of epinephrine-storing cells, while, on the surface of norepinephrine-storing cells, nicotinic receptors are primarily present.

4.6. Methodological limitations

We locally administered neostigmine to adrenal medulla through dialysis probe. Cholinesterase inhibitor was necessary to detect acetylcholine even during splanchnic nerve stimulation because released acetylcholine is rapidly